Inorganic Chemistry

Article

pubs.acs.org/IC

Electronic and Steric Influences of Pendant Amine Groups on the Protonation of Molybdenum Bis(dinitrogen) Complexes

Liezel A. Labios,[‡] Zachariah M. Heiden,[†] and Michael T. Mock*[,‡]

[‡]Center for Molecular Electrocatalysis, Physical Sciences Division, Pacific Northwest National Laboratory, Richland, Washington 99352, United States

[†]Department of Chemistry, Washington State University, Pullman, Washington 99164, United States

Supporting Information

ABSTRACT: The synthesis of a series of $P^{Et}P^{NRR'}$ ($P^{Et}P^{NRR'}$ = $Et_2PCH_2CH_2P(CH_2NRR')_2$, R = H, R′ = Ph or 2,4-difluorophenyl; R = R′ = Ph or ^{i}Pr) diphosphine ligands containing mono- and disubstituted pendant amine groups and the preparation of their corresponding molybdenum bis(dinitrogen) complexes *trans*-$Mo(N_2)_2(PMePh_2)_2(P^{Et}P^{NRR'})$ is described. In situ IR and multinuclear NMR spectroscopic studies monitoring the stepwise addition of triflic acid (HOTf) to *trans*-$Mo(N_2)_2(PMePh_2)_2(P^{Et}P^{NRR'})$ complexes in tetrahydrofuran at −40 °C show that the electronic and steric properties of the R and R′ groups of the pendant amines influence whether the complexes are protonated at Mo, a pendant amine, a coordinated N_2 ligand, or a combination of these sites. For example, complexes containing monoaryl-substituted pendant amines are protonated at Mo and the pendant amine site to generate mono- and dicationic Mo−H species. Protonation of the complex containing less basic diphenyl-substituted pendant amines exclusively generates a monocationic hydrazido ($Mo(NNH_2)$) product, indicating preferential protonation of an N_2 ligand. Addition of HOTf to the complex featuring more basic diisopropyl amines primarily produces a monocationic product protonated at a pendant amine site, as well as a trace amount of dicationic $Mo(NNH_2)$ product that is additionally protonated at a pendant amine site. In addition, *trans*-$Mo(N_2)_2(PMePh_2)_2(depe)$ (depe = $Et_2PCH_2CH_2PEt_2$) was synthesized to serve as a counterpart lacking pendant amines. Treatment of this complex with HOTf generated a monocationic $Mo(NNH_2)$ product. Protonolysis experiments conducted on several complexes in this study afforded trace amounts of NH_4^+.

Computational analysis of *trans*-$Mo(N_2)_2(PMePh_2)_2(P^{Et}P^{NRR'})$ complexes provides further insight into the proton affinity values of the metal center, N_2 ligand, and pendant amine sites to rationalize differences in their reactivity profiles.

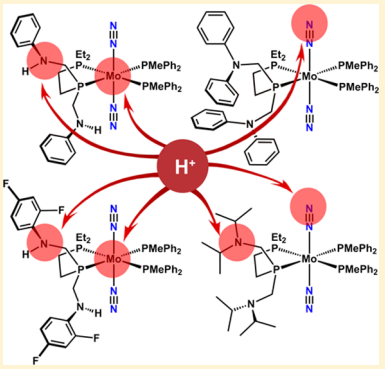

INTRODUCTION

Mo and W bis(dinitrogen) complexes containing phosphine ligands have received significant attention for their ability to serve as platforms to study dinitrogen reduction to ammonia.[1,2] When treated with Brønsted acids, complexes of the formulation $[M(N_2)_2(P)_4]$ (M = Mo, W; P = monodentate phosphine) afford ammonia and, in some cases, hydrazine.[3] In contrast, complexes bearing traditional diphosphine ligands $[M(N_2)_2(P{-}P)_2]$; (P−P = diphosphine; Figure 1, structure A) generally do not produce ammonia upon treatment with acid. Instead, conversion to the cationic metal−hydrazido complex $[M(NNH_2)X(P{-}P)_2]^+$ is commonly observed, which is a stable and well-characterized product from these reactions.[4] Notable exceptions to these observations are the diphosphine-bearing $M(N_2)_2(depf)_2$, $M(N_2)_2(bmpc)_2$, and $M(N_2)_2(depr)_2$ complexes (M = Mo, W; depf = 1,1′-bis(diethylphosphine)-ferrocene; bmpc = 1,1′-bis(dimethylphosphino)chromium; depr = 1,1′-bis(diethylphosphine)ruthenocene) reported by Nishibayashi and co-workers; their ability to produce ammonia during reactions with excess Brønsted acids demonstrates how modifying the diphosphine ligand structure by incorporating metallocene groups can lead to stoichiometric reduction of N_2 to ammonia.[5−7] Indeed, molecular catalysts that reduce N_2 to ammonia upon the addition of protons and electrons are highly sensitive to the design of the supporting ligand platform as well as the experimental conditions employed.[8,9]

Recent efforts in our group have focused on designing ligands that can mediate proton movement in N_2 reduction reactions. Specifically, our goals are to predict and control the movement of protons by tuning the steric and electronic properties of pendant amine groups in the second coordination sphere of group 6 bis(dinitrogen) complexes to influence the formation of protonated products in reactions with protic reagents and to determine if the pendant bases can facilitate proton movement to enhance stoichiometric NH_3 production. Previously, we reported that reactions of *trans*-$[Cr(N_2)_2(P^{Ph}{}_4N^{Bn}{}_4)]$ (Ph = phenyl, Bn = benzyl) with triflic acid (HOTf) in tetrahydrofuran (THF) at −50 °C generated $N_2H_5^+$ and NH_4^+.[10] Additionally, the pendant amine-containing

Received: January 28, 2015

DOI: 10.1021/acs.inorgchem.5b00209
Inorg. Chem. XXXX, XXX, XXX−XXX

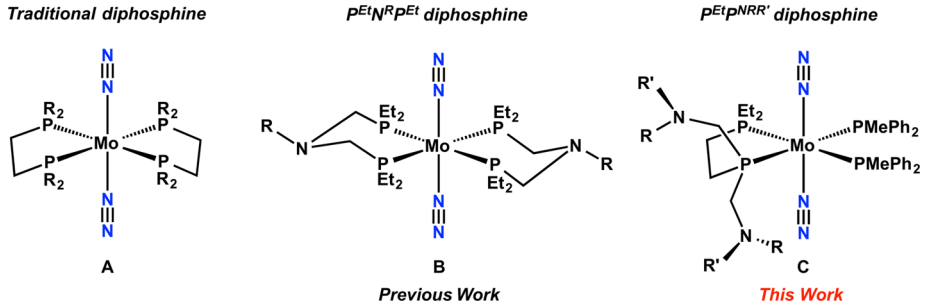

Figure 1. Mo bis(dinitrogen) complexes containing a traditional diphosphine ligand (A), $P^{Et}N^{R}P^{Et}$ diphosphine (B), and $P^{Et}P^{NRR'}$ diphosphine (C).

complex *trans*-$[W(N_2)_2(dppe)(P^{Et}N^{Me}P^{Et})]$ (dppe = $Ph_2PCH_2CH_2PPh_2$; $P^{Et}N^{Me}P^{Et}$ = $Et_2PCH_2N(Me)CH_2PEt_2$) yielded more NH_4^+ (0.81 equiv) in reactions with excess HOTf than its counterpart that lacks a pendant amine, *trans*-$[W(N_2)_2(dppe)(depp)]$ (depp = $Et_2PCH_2CH_2CH_2PEt_2$), which formed 0.40 equiv of NH_4^+.[11] Such a result is notable since it suggests that the pendant amine group may play a role in the stoichiometric formation of ammonia.

Reactions of *trans*-$[W(N_2)_2(dppe)(P^{Et}N^{Me}P^{Et})]$ with stoichiometric amounts of HOTf also produced seven-coordinate tungsten-hydride products (i.e., *trans*-$[W(H)(N_2)_2(dppe)(P^{Et}N^{Me}P^{Et})]^+$), which could undergo subsequent protonation at the pendant amine site upon treatment with additional equivalents of acid. Spectroscopic data revealed that initial protonation at the metal center and at the pendant amine sites ultimately destabilizes N_2 coordination. Thus, we reasoned that formation of these products are obstacles to promoting N_2 reduction.

To gain insight into the formation of metal hydride products and ultimately to preclude formation of these products, we examined the reactivity patterns of *trans*-$[Mo(N_2)_2(P^{Et}N^{R}P^{Et})_2]$ complexes (Figure 1, structure B) in the presence of stoichiometric amounts of HOTf.[12] The supporting ligands in these complexes feature pendant amines with various substituents (R = Ph, 2,6-difluorobenzyl, 3,5-difluorobenzyl, $CH_2CH_2NMe_2$, CH_2-*o*-Py). Our findings provided preliminary experimental evidence that the complexes containing less basic pendant amines were more likely to be protonated at the N_2 ligands and generated greater ratios of $Mo(NNH_2)$ to $Mo(H)(N_2)$ products. Herein we present the synthesis of a series of Mo-bis(dinitrogen) complexes with diphosphine ligands featuring pendant amines that are not incorporated into the ligand backbone, (Figure 1, structure C). In this study, we describe how the steric and electronic properties of pendant amine groups as the terminal substituents on one of the chelating phosphorus atoms affect which sites are protonated upon treatment with acid. Additionally, we elucidate which factors promote protonation of the dinitrogen moiety in these $Mo(N_2)_2$ complexes.

RESULTS AND DISCUSSION

Synthesis and Characterization of *trans*-[Mo(N$_2$)$_2$(PMePh$_2$)$_2$(P^{Et}P$^{NRR'}$)] Complexes. Precursors of the target ligands were synthesized by hydrophosphination of diethyl vinylphosphonate with diethylphosphine in the presence of azobisisobutyronitrile (AIBN) at 65 °C to generate the phosphonate $Et_2PCH_2CH_2P(O)(OEt)_2$, followed by reduction with $LiAlH_4$ (Scheme 1). Treatment of the resulting diphosphine, $Et_2PCH_2CH_2PH_2$, with 2 equiv of paraformaldehyde, $(CH_2O)_n$, and subsequent condensation with a primary or secondary amine afforded the corresponding $P^{Et}P^{NRR'}$ (PP^N) ligands ($P^{Et}P^{NRR'}$ = $Et_2PCH_2CH_2P(CH_2NRR')_2$, R = H, R′ = Ph ($P^{Et}P^{NH(Ph)}$); R = H, R′ = 2,4-difluorophenyl ($P^{Et}P^{NH(ArF2)}$); R = R′ = Ph ($P^{Et}P^{N(Ph)2}$); R = R′ = ^{i}Pr ($P^{Et}P^{N(iPr)2}$)). The installation of mono- and diaryl-substituted pendant amines in $P^{Et}P^{NH(Ph)}$, $P^{Et}P^{NH(ArF2)}$, and $P^{Et}P^{N(Ph)2}$ represents an effort to achieve closer matching of the pK_a values of the protonated pendant amines and dinitrogen ligands in the desired Mo complexes (see below). Computational results recently reported by our group suggested that pK_a matching between these two kinetically favored protonation sites will be important to facilitate the protonation of the N_2 ligands, rather than the metal center or the pendant amines.[11] As we previously observed, addition of HOTf to $M(N_2)$ (M = Cr, Mo, W, Fe) phosphine complexes containing basic alkyl substituted pendant amine groups afforded a mixture of protonated

Scheme 1. Synthesis of $P^{Et}P^{NRR'}$ Ligands

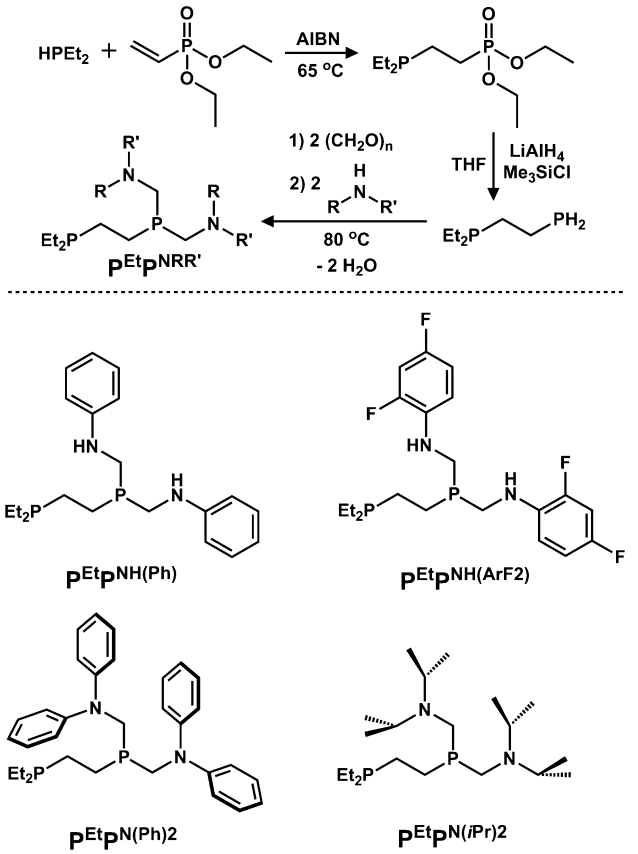

DOI: 10.1021/acs.inorgchem.5b00209
Inorg. Chem. XXXX, XXX, XXX−XXX

products.[10−13] For example, treatment of *trans*-[$W(N_2)_2$-(dppe)($P^{Et}N^{Me}P^{Et}$)] with HOTf at −78 to −40 °C generated tungsten complexes protonated at the metal center and at the pendant amine sites, as well as at the N_2 ligands.[11] In addition to electronically tuning the pendant amines and liberating them from the constraints of the ligand backbone to promote proton delivery exclusively to the N_2 ligands, we reasoned that steric modifications were necessary to inhibit proton transfer to the metal center. Accordingly, $P^{Et}P^{N(iPr)2}$, which is a sterically similar counterpart of $P^{Et}P^{N(Ph)2}$ that contains more basic pendant amine groups, is examined in the present study.

Synthetic access to isolable $Mo(N_2)$ complexes with $P^{Et}P^{NRR'}$ ligands was difficult to achieve via chemical reductions of high-valent MoX (X = Cl, Br) precursors, such as $MoCl_5$ and $MoBr_3(THF)_3$. These methods have generally been effective with a variety of mono-, bi-, and tridentate phosphine ligands (L) to generate zerovalent $Mo(N_2)_m(L)_n$ complexes.[14] However, these reduction reactions in the presence of the $P^{Et}P^{NRR'}$ diphosphine ligands produced dark brown intractable mixtures. Consequently, the zerovalent bis(dinitrogen) complex *trans*-$Mo(N_2)_2(PMePh_2)_4$ was employed as a synthetic precursor, since it has been reported to serve as a convenient coordination platform for phosphorus, nitrogen, and sulfur donors.[15] Substitution of two $PMePh_2$ ligands in *trans*-$Mo(N_2)_2(PMePh_2)_4$ upon addition of 1.2 equiv of the chelating $P^{Et}P^{NRR'}$ ligands in ethereal solvents afforded the respective *trans*-$Mo(N_2)_2(PMePh_2)_2(P^{Et}P^{NRR'})$ complexes ($P^{Et}P^{NRR'}$ = $P^{Et}P^{NH(Ph)}$ (**1**), $P^{Et}P^{NH(ArF2)}$ (**2**), $P^{Et}P^{N(Ph)2}$ (**3**), $P^{Et}P^{N(iPr2)}$ (**4**), Scheme 2) as red oils due to the presence of nonvolatile free

Scheme 2[a]

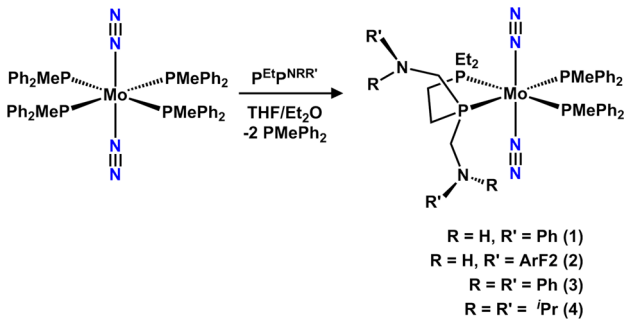

[a]Synthesis of *trans*-$Mo(N_2)_2(PMePh_2)_2(P^{Et}P^{NH(Ph)})$ (**1**), *trans*-$Mo(N_2)_2(PMePh_2)_2(P^{Et}P^{NH(ArF2)})$ (**2**), *trans*-$Mo(N_2)_2(PMePh_2)_2(P^{Et}P^{N(Ph)2})$ (**3**), and *trans*-$Mo(N_2)_2(PMePh_2)_2(P^{Et}P^{N(iPr)2})$ (**4**).

phosphines in the crude product mixtures. In the synthetic workups of **1**, **2**, and **4**, the addition of CuCl[16] was effective to remove free phosphines from the reaction mixtures. Subsequent purification through a short column of neutral alumina afforded the Mo bis(dinitrogen) complexes as bright orange solids. Additionally, efforts to substitute a second $P^{Et}P^{NRR'}$ ligand onto each of these complexes to produce *trans*-$Mo(N_2)_2(P^{Et}P^{NRR'})_2$ compounds were unsuccessful. For example, heating THF solutions of *trans*-$Mo(N_2)_2(PMePh_2)_2$-($P^{Et}P^{NRR'}$) complexes in the presence of excess $P^{Et}P^{NRR'}$ ligand at 60 °C for 4 h generated mixtures of unidentified products.

Complexes **1**−**4** were structurally characterized by single-crystal X-ray diffraction, and their molecular structures are depicted in Figure 2. The N≡N bond distances in **1**−**4** (1.121(4) Å average (av)) are elongated compared to that of free N_2 (1.0975 Å).[17] Additionally, the solid-state antisymmetric ν(N≡N) stretches (1930−1941 cm^{-1}, KBr) are consistent with activation of the N_2 ligand upon coordination to Mo and are comparable to those of other zerovalent Mo-phosphine bis(dinitrogen) complexes.[14c,15a,18] The $^{15}N_2$-labeled isotopologues *trans*-$Mo(^{15}N_2)_2(PMePh_2)_2(P^{Et}P^{NRR'})$ (**1**-($^{15}N_2$)$_2$−**4**($^{15}N_2$)$_2$) were prepared in situ in an NMR tube by sonication of **1**−**4** in THF-d_8 under an atmosphere of $^{15}N_2$ gas for 3 h. Resonances in the $^{15}N\{^1H\}$ NMR spectra corresponding to the proximal nitrogen atoms (N_α) are multiplets at $\delta \approx -39$ while those of the distal nitrogen atoms (N_β) are doublets (J_{NN} = 5−6 Hz) at $\delta \approx -42$. The phosphorus atoms (P1) geminal to the pendant amines in **1**−**4** exhibit $^{31}P\{^1H\}$ NMR chemical shifts that reflect the relative basicities of the pendant amines. The $^{31}P\{^1H\}$ NMR resonance for **4**, which contains the most basic pendant amine groups, is located more upfield at δ 50.7, whereas those of **1** and **2**, which contain phenyl substituents, appear at δ 60.8 and 61.5, respectively. The most downfield $^{31}P\{^1H\}$ NMR resonance (δ 77.0) is observed for **3**, which contains the least basic pendant amines.

It is also important to highlight some structural differences between the $P^{Et}P^{NRR'}$ ligands presented in this study versus the bidentate PNP ligands (vide supra) in the group 6 metal-bis(dinitrogen) complexes that have previously been studied in our laboratory.[10−13,19] For example, the pendant amines in the PNP ligand scaffolds are constrained within the phosphine ligand backbone, whereas those in the $P^{Et}P^{NRR'}$ ligands are the terminal substituents on one of the chelating phosphorus atoms and exhibit greater flexibility. This structural modification may help facilitate proton delivery from the pendant amines to the dinitrogen ligands. As illustrated in Figure 2, the molecular structures of **1** and **2** both reveal the positioning of a pendant amine N−H group toward an N_2 moiety. These hydrogen atoms (H6) are located in the electron density difference map 2.75(2) Å and 2.76(2) Å from a distal nitrogen atom (N2) in **1** and **2**, respectively. The N2−H6 distances are slightly greater than the sum of the van der Waals (vdW) radii between these atoms (r_{vdW}(H) + r_{vdW}(N) = 2.59−2.74 Å)[20] and may illustrate the potential for a protonated pendant amine to facilitate intramolecular proton transfer in solution. In the infrared spectra (KBr), ν(N−H) bands appear at 3401 and 3368 cm^{-1} for **1**, and at 3396 and 3322 cm^{-1} for **2**. Other notable structural features include the increased distances between the pendant amines and Mo atoms crystallographically observed in **3** and **4** (4.67−4.98 Å) compared to those in *trans*-$Mo(N_2)(PNP)_2$ complexes (4.05(3) Å av).[12,19b] These distances reflect the greater steric profiles of the pendant amines in **3** and **4**, which are expected to inhibit intramolecular proton transfer to the metal center and thus preclude the formation of Mo-hydride products in the presence of acid.

Protonation Studies of *trans*-[$Mo(N_2)_2(PMePh_2)_2$-($P^{Et}P^{NRR'}$)] Complexes with HOTf. In situ IR and multinuclear NMR spectroscopic experiments were conducted to probe how the electronic and steric features of the pendant amine groups in the $P^{Et}P^{NRR'}$ ligands influence the reactivity of complexes **1**−**4** toward acid. Treatment of THF solutions of **1** and **2** at −40 °C (ν(N≡N) = 1939 and 1947 cm^{-1}, respectively) with 1 equiv of HOTf afforded the corresponding seven-coordinate monocationic Mo(II) hydrides, *trans*-[Mo-

DOI: 10.1021/acs.inorgchem.5b00209
Inorg. Chem. XXXX, XXX, XXX−XXX

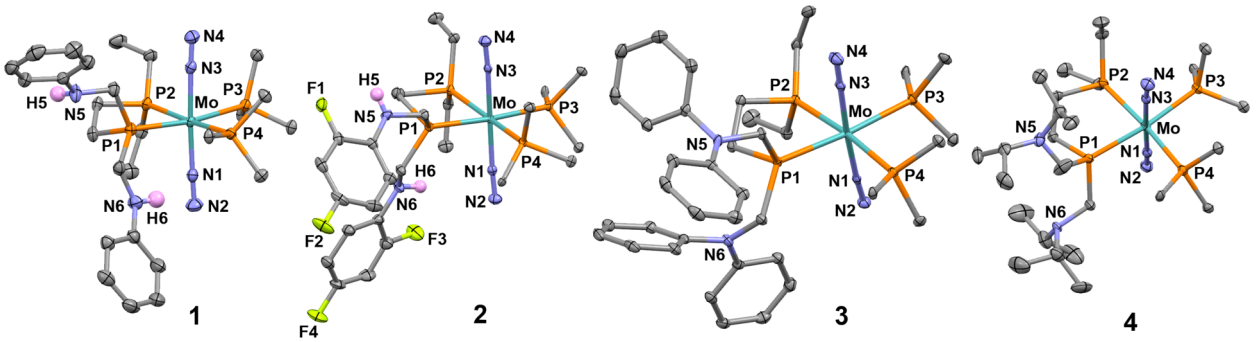

Figure 2. Molecular structures of *trans*-$Mo(N_2)_2(PMePh_2)_2(P^{Et}P^{NH(Ph)})$ (**1**), *trans*-$Mo(N_2)_2(PMePh_2)_2(P^{Et}P^{NH(ArF2)})$ (**2**), *trans*-$Mo(N_2)_2(PMePh_2)_2(P^{Et}P^{N(Ph)2})$ (**3**), and *trans*-$Mo(N_2)_2(PMePh_2)_2(P^{Et}P^{N(iPr)2})$ (**4**). Thermal ellipsoids are drawn at 50% probability. Only the C_{ipso} atoms of the phenyl groups on the $PMePh_2$ ligands are shown. All hydrogen atoms, except for those in the N−H moieties of **1** and **2**, are omitted for clarity.

$(H)(N_2)_2(PMePh_2)_2(P^{Et}P^{NH(Ph)})](OTf)$ ($[\mathbf{1H}]^+$) and *trans*-$[Mo(H)(N_2)_2(PMePh_2)_2(P^{Et}P^{NH(ArF2)})](OTf)$ ($[\mathbf{2H}]^+$), respectively (Scheme 3). $[\mathbf{1H}]^+$ and $[\mathbf{2H}]^+$ each exhibit a

Scheme 3. Stepwise Protonation of 1 and 2 with HOTf

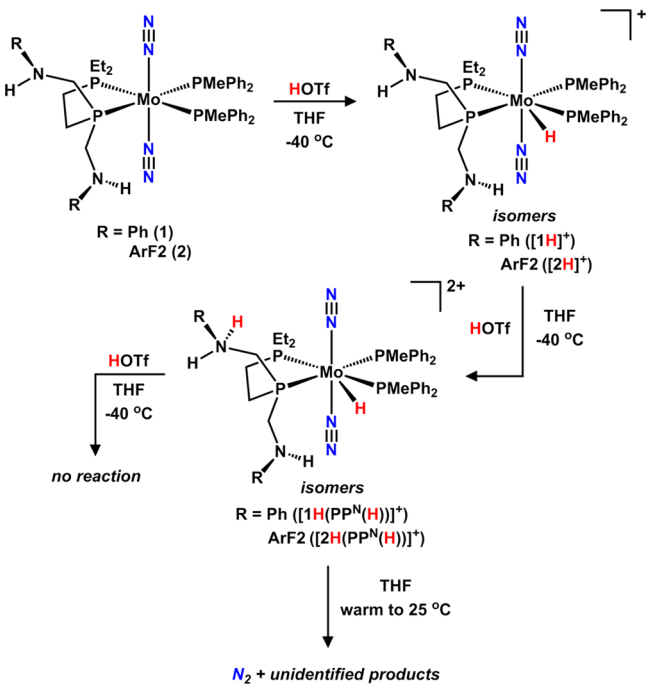

$\nu(N{\equiv}N)$ band at 2024 cm^{-1} (Figure 3a,b), which is ~80 cm^{-1} higher in energy and reflects decreased π-backbonding from Mo to the N_2 ligands due to protonation of the metal center. Addition of a second equivalent of HOTf results in an increase of the $\nu(N{\equiv}N)$ vibrational frequencies by 20 cm^{-1}, consistent with protonation of a pendant amine site to generate the dicationic Mo(II) hydrides, *trans*-$[Mo(H)(N_2)_2(PMePh_2)_2(P^{Et}P^{NH(Ph)}(H))](OTf)_2$ ($[\mathbf{1H(PP^N(H))}]^{2+}$, $\nu(N{\equiv}N)$ = 2044 cm^{-1}) and *trans*-$[Mo(H)(N_2)_2(PMePh_2)_2(P^{Et}P^{NH(ArF2)}(H))](OTf)_2$ ($[\mathbf{2H(PP^N(H))}]^{2+}$, $\nu(N{\equiv}N)$ = 2046 cm^{-1}) (Scheme 3 and Figure 3a,b). The $\nu(N{\equiv}N)$ stretches of $[\mathbf{1H(PP^N(H))}]^{2+}$ and $[\mathbf{2H(PP^N(H))}]^{2+}$ persisted even after subsequent treatment with additional equivalents of HOTf, indicating that further protonation of the Mo complexes did not occur (Scheme 3).

While the ν(Mo−H) bands of the mono- and dicationic hydride complexes could not be identified within the in situ IR spectra, two sets of multiplets corresponding to the Mo−H functionalities were observed by ^1H NMR spectroscopy (Figure 4). Additionally, $^{15}N\{^1H\}$ NMR spectra monitoring the stepwise addition of HOTf to cooled (−40 °C) THF-d_8 solutions of the $^{15}N_2$-containing analogues $\mathbf{1}(^{15}\mathbf{N_2})_2$ and $\mathbf{2}(^{15}\mathbf{N_2})_2$ exhibit two pairs of signals for the corresponding hydride ($[\mathbf{1H}(^{15}\mathbf{N_2})_2]^+$ and $[\mathbf{2H}(^{15}\mathbf{N_2})_2]^+$) and protonated hydride ($[\mathbf{1H}(^{15}\mathbf{N_2})_2(\mathbf{PP^N(H)})]^{2+}$ and $[\mathbf{2H}(^{15}\mathbf{N_2})_2(\mathbf{PP^N(H)})]^{2+}$) products, respectively (Figure 4). Two sets of $^{31}P\{^1H\}$ resonances are also present after each protonation step (Figures S3 and S6, Supporting Information). These observations are consistent with the formation of two hydride isomers in both reactions, which may be a result of the asymmetric nature of the molecule since seven-coordinate complexes typically exhibit fluxional behavior in solution.[21]

The susceptibility of the metal centers and pendant amines in **1** and **2** toward protonation suggests several possibilities. First, these pendant amines are sufficiently more basic than the N_2 ligands and are thermodynamically favored for protonation (see Computational Analysis). Moreover, the monoaryl-substituted pendant amines lack the steric bulk that could potentially inhibit proton transfer to the metal center, which is the thermodynamically favored protonation site.[22] Protonation at the metal center is problematic in this system because $Mo(H)(N_2)$ complexes are less likely to be protonated at the N_2 ligands.[23] As illustrated by the in situ IR experiments above, protonation at the metal center consequently causes decreased π-backbonding to the N_2 ligands. This results in both decreased basicity and increased lability of the N_2 ligands. The increased charge of the $Mo(H)(N_2)$ cation would also result in a less basic N_2 site. Consistent with this description, the mono- and dicationic Mo hydride complexes in this study were observed to dissociate N_2 upon warming to room temperature (Scheme 3).

Next, we examined the reactivity of **3**, which contains sterically encumbering diphenyl-substituted pendant amines. In situ IR experiments monitoring the treatment of **3** with 1 equiv of HOTf in THF at −40 °C resulted in a decrease in intensity of the $\nu(N \equiv N)$ band at 1943 cm^{-1} (Figure 3c). ^{31}P and ^1H NMR spectra of this reaction revealed a mixture of **3** and the Mo-hydrazido complex *trans*-$[Mo(NNH_2)(OTf)(PMePh_2)_2(P^{Et}P^{N(Ph)2})](OTf)$ ($[\mathbf{3(NNH_2)}]^+$), in ~1:1 ratio. Notably, a Mo hydride product was not formed. Upon addition of the second equivalent of HOTf, the $\nu(N \equiv N)$ band immediately disappeared, indicating that 2 equiv of HOTf are necessary for

DOI: 10.1021/acs.inorgchem.5b00209
Inorg. Chem. XXXX, XXX, XXX−XXX

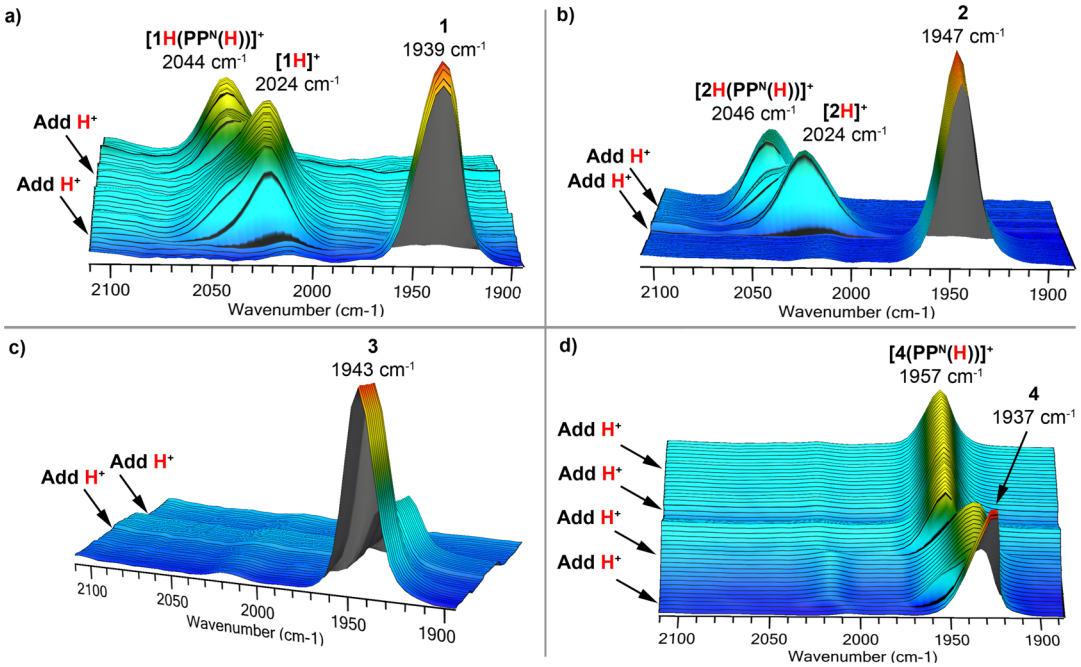

Figure 3. In situ IR plots recorded in THF at −40 °C from the reaction of complexes **1**−**4** with HOTf.

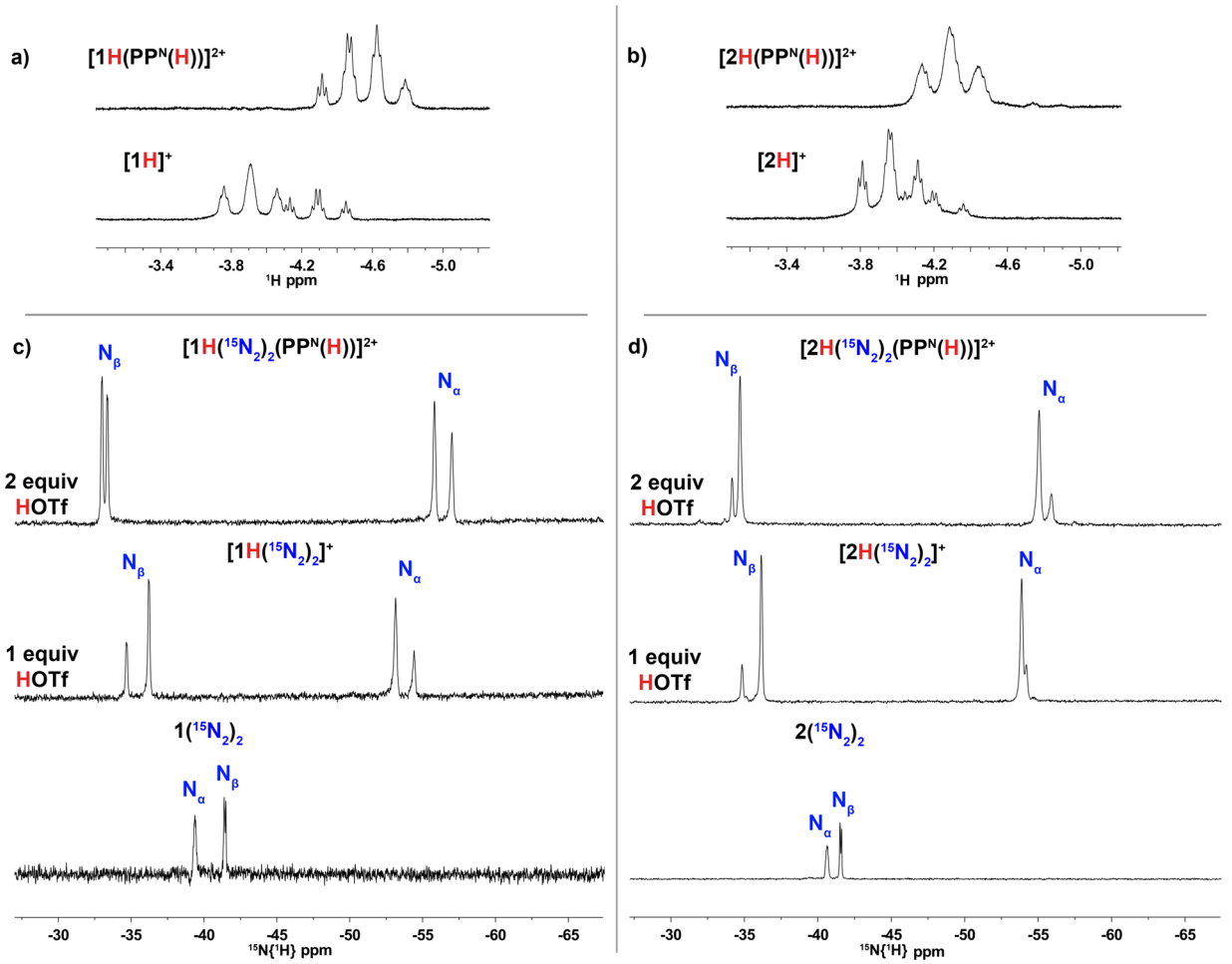

Figure 4. ^{1}H NMR spectra of **1** (a) and **2** (b) and corresponding ^{15}N{^{1}H} NMR spectra of **1** (c) and **2** (d) recorded in THF-d_8 at −40 °C monitoring the stepwise protonation with HOTf.

DOI: 10.1021/acs.inorgchem.5b00209
Inorg. Chem. XXXX, XXX, XXX−XXX

Scheme 4. Protonation of 3 with HOTf

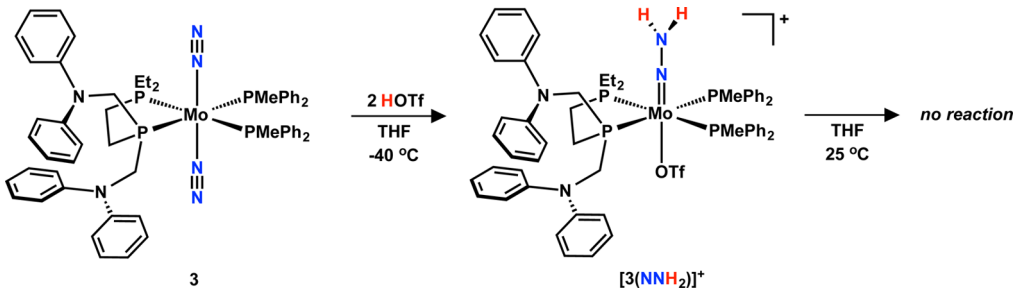

the complete conversion of **3** to $[\mathbf{3}(\mathbf{NNH_2})]^+$, which persists upon warming to room temperature (Scheme 4). The $^1H-^{15}N$ HMBC spectrum of $[\mathbf{3}(^{15}\mathbf{N}^{15}\mathbf{NH_2})]^+$, prepared by protonation of $\mathbf{3}(^{15}\mathbf{N_2})_2$ with 2 equiv of HOTf, exhibits a correlation between the hydrazido protons (9.45 ppm, d, J_{NH} = 91.3 Hz) and ^{15}N resonances at δ −46.1 (m, N_α) and δ −216.9 (d, J_{NN} = 10.3 Hz, N_β). These spectroscopic features are consistent with those reported for analogous Mo and W hydrazido complexes.[24] The infrared spectrum of $[\mathbf{3}(\mathbf{NNH_2})]^+$ exhibits ν(N−H) bands at 3312, 3249, and 3129 cm^{-1} (KBr). The presence of three ν(N−H) stretches is attributed to intermolecular H-bonding interactions between the hydrazido protons and the outer sphere OTf^- counteranions in the solid state.[25] Crystallographic characterization of $[\mathbf{3}(\mathbf{NNH_2})]^+$ revealed a distance of 2.11(3) Å between a hydrogen atom on the NNH_2 group of one molecule and an OTf^- counteranion of another $[\mathbf{3}(\mathbf{NNH_2})]^+$ molecule in the crystal lattice (Figure 5). The ν(N−N) vibrational frequency, which is expected to occur within the 1300−1500 cm^{-1} region,[24a,25c,26] could not be observed due to overlapping features corresponding to the free OTf^- counteranion. The metric parameters exhibited by the molecular structure of $[\mathbf{3}(\mathbf{NNH_2})]^+$ include an elongated N−N bond distance (1.308(2) Å) relative to the parent bis(dinitrogen) complex, **3** (1.125(4) Å, av), and a shortened Mo−N bond distance (1.741(1) Å vs 2.017(8) Å, av). Other reported examples of structurally characterized molybdenum- and tungsten-hydrazido complexes exhibit N−N bond lengths closer to an order of 1.5, with considerable multiple bonding between the metal and the hydrazido ligand.[4b,27]

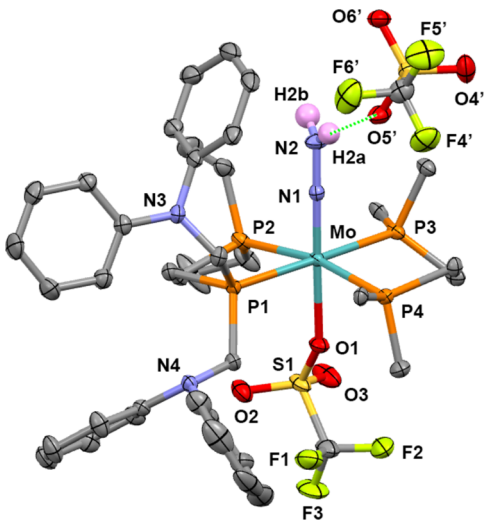

Figure 5. Molecular structure of *trans*-$[Mo(NNH_2)(OTf)(PMePh_2)_2(P^{Et}P^{N(Ph)2})](OTf)$ ($[\mathbf{3}(\mathbf{NNH_2})]^+$). Thermal ellipsoids are drawn at 50% probability. Only the C_{ipso} atoms of the phenyl groups on the $PMePh_2$ ligands are shown. All hydrogen atoms, except for those in the NNH_2 group, are omitted for clarity. An OTf^- counteranion from another molecule in the crystal lattice is included to illustrate the intermolecular H-bonding interaction with a hydrogen atom of the NNH_2 group.

While the stepwise protonation of **1** and **2** generated Mo hydride products, the protonation of **3** with HOTf exclusively generated $[\mathbf{3}(\mathbf{NNH_2})]^+$. This result prompted us to examine whether the steric environment of the pendant amines indeed plays a role in preventing the formation of Mo−H species, and whether the diphenyl groups provided sufficient pK_a matching between the pendant amines and N_2 ligands. Accordingly, stepwise protonation experiments were performed on **4**, which contains diisopropyl pendant amine groups that are both sterically encumbering and the most basic of the series. In situ IR experiments in THF at −40 °C revealed a shift of the ν(N≡N) band from 1937 to 1942 cm^{-1} upon addition of 1 equiv of HOTf to **4**, with a subsequent shift to 1957 cm^{-1} in the presence of 2 equiv of HOTf (Figure 3d). The latter shift of the ν(N≡N) band is consistent with protonation at a pendant amine site to afford the monocationic complex *trans*-$[Mo(N_2)(PMePh_2)_2(P^{Et}P^{N(iPr)2}(H))](OTf)$ ($[\mathbf{4}(\mathbf{PP^N(H)})]^+$, Scheme 5). Remarkably, protonation of a pendant amine without prior protonation of the metal center is unprecedented in our study of Mo and W dinitrogen complexes supported by phosphine ligands containing pendant amine groups. These results suggest that the steric bulk and high basicity of the isopropyl substituents prevent formation of a Mo−H product. Spectral features corresponding to a Mo-hydride functionality were not observed in the NMR and IR spectra for this reaction. The ^{31}P NMR resonances for $[\mathbf{4}(\mathbf{PP^N(H)})]^+$ are broadened compared to the starting complex **4**, and only minor changes in chemical shift are observed (Figure S9, Supporting Information). Notably, the $^{15}N\{^1H\}$ NMR spectrum of $[\mathbf{4}(^{15}\mathbf{N_2})_2(\mathbf{PP^N(H)})]^+$ recorded at −40 °C contains only a single resonance for the proximal and distal nitrogen atoms of N_2 ligand (Figure S10, Supporting Information), compared to separate resonances that are observed for the N_2 ligands in $\mathbf{4}(^{15}\mathbf{N_2})_2$. In addition to the formation of $[\mathbf{4}(^{15}\mathbf{N_2})_2(\mathbf{PP^N(H)})]^+$, the $^1H-^{15}N$ HMBC spectrum exhibits crosspeaks corresponding the Mo hydrazido product, *trans*-$[Mo(NNH_2)(OTf)(PMePh_2)_2(P^{Et}P^{N(iPr)2})](OTf)$ ($[\mathbf{4}(^{15}\mathbf{N}^{15}\mathbf{NH_2})(\mathbf{PP^N})]^+$, Scheme 5) which is present only in a trace amount based on integration of ^1H NMR spectra.

Despite the highly basic nature of the pendant amines in **4**, no further shift of the ν(N≡N) band was observed when an additional 2 equiv of HOTf were added, indicating that a second protonation event at the pendant amine site of

DOI: 10.1021/acs.inorgchem.5b00209
Inorg. Chem. XXXX, XXX, XXX−XXX

Scheme 5. Stepwise Protonation of 4 with HOTf

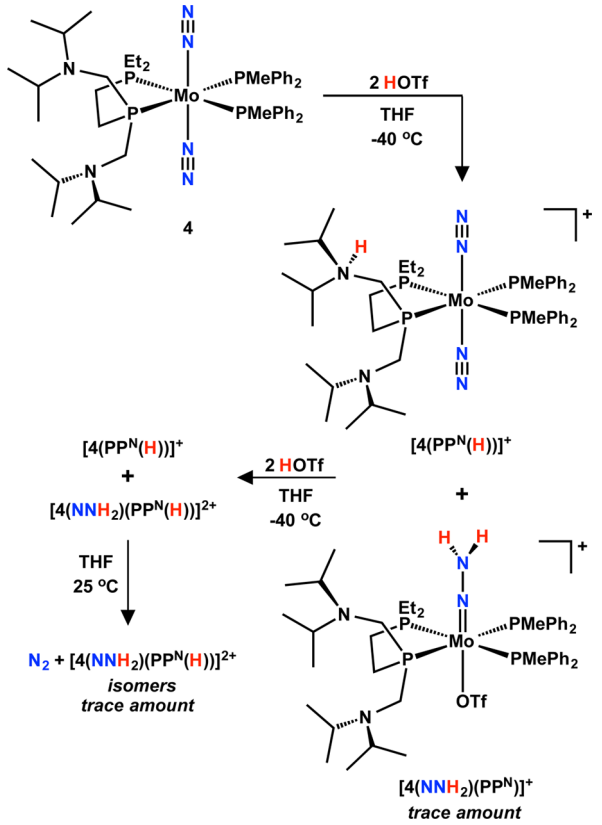

Scheme 6. Synthesis of 5 and the Protonation of 5 with HOTf

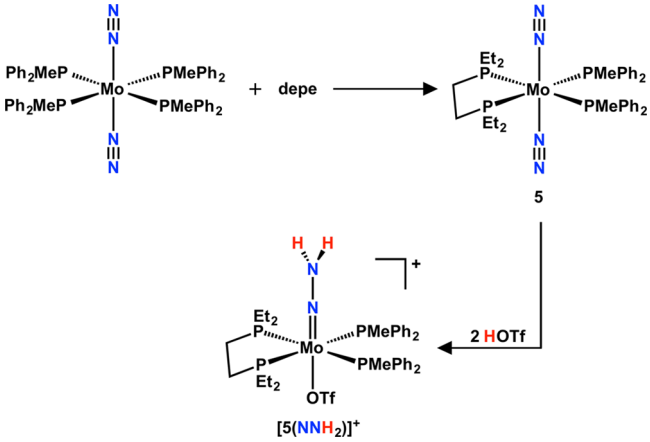

([**4**(**PP**$^{\mathbf{N}}$(**H**))]$^{+}$) does not occur. This contrasts our previously reported studies of Cr, Mo, and Fe complexes containing two alkyl- or benzyl-substituted pendant amines, in which both basic pendant amine sites, as well as the metal center, are protonated in the presence of excess acid.[10,12,13] The ^{1}H−^{15}N HMBC spectrum of the reaction mixture after an additional 2 equiv of HOTf was added exhibits crosspeaks corresponding to two Mo hydrazido products, presumably isomers of *trans*-[Mo(NNH$_2$)(OTf)(PMePh$_2$)$_2$(P^{Et}P$^{N(iPr)2}$(H))](OTf)$_2$ ([**4**(**NNH$_2$**)(**PP**$^{\mathbf{N}}$(**H**))]$^{2+}$, Scheme 5) with the protonated pendant amine positioned near either the metal-bound NNH$_2$ or OTf^{-} ligand. This result is similar to the tungsten hydrazido isomers protonated at a pendant amine reported in a recent study from our group.[11] We reason that protonation of both pendant amines in **4** is unlikely due to their close proximity to each other on the same ligand. ([**4**(**PP**$^{\mathbf{N}}$(**H**))]$^{+}$ was found to be quite temperature-sensitive. Increasing the temperature of the solution above −40 °C for only 1−2 min resulted in dissociation of the N$_2$ ligands. In contrast, [**4**(**^{15}N^{15}NH$_2$**)(**PP**$^{\mathbf{N}}$(**H**))]$^{2+}$ persists in solution at room temperature (Scheme 5).

This series of reactivity studies demonstrates that the pendant amines in **3** exhibit a combination of basicity and steric encumbrance to promote exclusive protonation at the N$_2$ ligand. For additional comparison, a complex without a pendant amine, *trans*-[Mo(N$_2$)$_2$(PMePh$_2$)$_2$(depe)] (**5**), (depe = Et$_2$PCH$_2$CH$_2$PEt$_2$) was prepared. The synthesis of **5** was conducted similarly to its pendant amine-containing analogues via a ligand-exchange reaction between *trans*-Mo(N$_2$)$_2$(PMePh$_2$)$_4$ and depe (Scheme 6). Treatment of **5** with 2 equiv of HOTf generated the corresponding hydrazido cation *trans*-[Mo(NNH$_2$)(OTf)(PMePh$_2$)$_2$(depe)](OTf) ([**5**(**NNH$_2$**)]$^{+}$), which is stable at room temperature. Crystals for X-ray diffraction studies were not obtained, yet the NMR and IR spectroscopic properties of [**5**(**NNH$_2$**)]$^{+}$ are consistent with those observed for [**3**(**NNH$_2$**)]$^{+}$. Reactions between molybdenum and tungsten bis(dinitrogen) complexes bearing conventional phosphine ligands (i.e., depe, dppe) with stoichiometric amounts of strong acid generally form the hydrazido containing products, and in some cases, hydrido-hydrazido complexes.[4b,23b] In the present case, however, reactions between **5** and HOTf did not generate Mo hydride products. It is worth comparing the acid reactivity of **5** with that of **1** and **2**, since the supporting ligands in each of these complexes offer less steric protection around Mo. The formation of Mo hydrides from stoichiometric protonation of both **1** and **2**, but not from protonation of **5**, suggests that the pendant amines may facilitate inter- or intramolecular proton delivery to the metal center.

Protonolysis Reactions for Ammonia Production. Exclusive protonation of the N$_2$ ligands in **3** and **5** prompted us to examine the reactivity of these complexes in the presence of excess acid. The reactivity of **1** toward excess acid was explored as well for comparison. Overall, very low yields of ammonia, 0.02−0.04 equiv per Mo, were detected by the indophenol method. Reaction conditions with excess HOTf in fluorobenzene at room temperature for 20 h similarly afforded 0.03, 0.02, and 0.04 equiv per Mo of ammonia for **1**, **3**, and **5**, respectively. To reproduce the conditions employed in the stoichiometric protonation experiments described above (which were monitored by in situ IR and NMR spectroscopy), reactions of these complexes with excess acid were conducted in THF at −40 °C for 10 min prior to reaction workup and analysis. The short reaction time was employed to avoid polymerization of THF in the presence of excess HOTf. However, neither these reactions nor those employing H$_2$SO$_4$ as acid produced more than trace amounts of ammonia. Hydrazine was also not detected in these reactions. Table S1 in the Supporting Information lists the reaction conditions that were explored and the resulting yields of ammonia from each reaction.

The poor yield of ammonia from protonolysis reactions featuring these Mo(N$_2$)$_2$ complexes, particularly **3** and **5**, is attributed to the stability of their hydrazido counterparts. For instance, no ammonia was observed upon treatment of [**3**(**NNH$_2$**)]$^{+}$ and [**5**(**NNH$_2$**)]$^{+}$ with HOTf. Thus, use of an

DOI: 10.1021/acs.inorgchem.5b00209
Inorg. Chem. XXXX, XXX, XXX−XXX

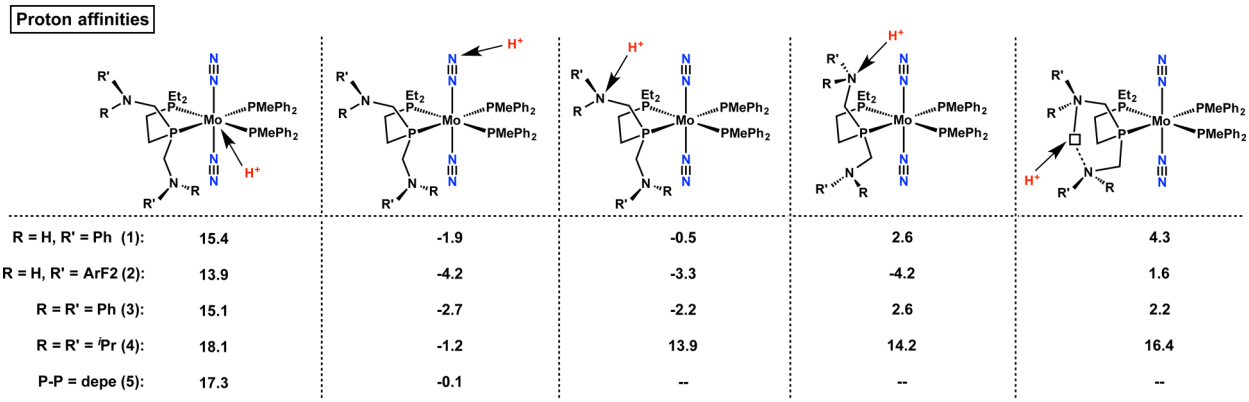

Figure 6. Computationally derived proton affinity values in kcal/mol for the metal center, N_2 ligand, and pendant amine site of complexes **1**−**5**.

external reductant is likely required to achieve further conversion of the NNH_2 moiety.

Computational Analysis. Computational analysis employing density functional theory (DFT)-based electronic structure methods was used to rationalize the thermodynamically preferred outcomes of the protonation studies. The computationally derived pK_a values in THF were converted to proton affinities (1.364 × pK_a) for complexes **1**−**5** and are summarized in Figure 6. Proton affinity values of the pendant amine sites were found to be dependent on the amine group orientation with respect to the formation of intramolecular N−H−N contacts with the opposing pendant amine or with the N−H directed toward the N_2 ligand. Molecular structures containing intramolecular N−H−N contacts are shown in the right two columns in Figure 6. In general, when intramolecular N−H−N contacts are observed in the optimized structures of the DFT calculations, the protons are stabilized, and the pendant amine exhibited more positive proton affinity values than complexes without the intramolecular contacts. Indeed, while an increase in proton affinity values for the pendant amine sites are noted in these structures, it is difficult to quantify if these interactions influence the reactivity of these complexes with acid. For the discussion below, we considered the proton affinity values for optimized structures that did not exhibit these types of intramolecular contacts.

Comparing the proton affinity values of the three possible protonation sites (N_2 ligand, pendant amine, and metal center) of **1** and **2** (which have the least sterically demanding pendant amine groups), computational analysis predicts the proton affinity of the metal center to be ∼17 kcal/mol more basic than the pendant amine sites. Meanwhile, the N_2 ligands are ∼1−2 kcal/mol less basic than the pendant amines, indicating that the metal center is the thermodynamically preferred site of protonation. Experimentally, the addition of 1 equiv of HOTf at −40 °C to complexes **1** and **2** afforded a Mo−H product as opposed to products that were protonated exclusively at the pendant amine or dinitrogen ligands. Because of the location of the amines in the second coordination sphere of the molecule, these sites in **1** and **2** are kinetically more accessible toward protonation than the metal center. Thermodynamically, in **1** and **2**, the amines are predicted to be better proton acceptors than the N_2 ligand. Because of their small steric profiles (as observed in the X-ray structure of **1** and **2** and by geometry-optimized DFT structures), a protonated amine can readily be positioned to point toward the metal center to deliver a proton.

In contrast to **1** and **2**, experimental results revealed the addition of acid to **3** results in exclusive protonation at the N_2 ligand. Additionally, the formation of a Mo−H product was not observed. The proton affinity of the metal center in complex **3** is 15.1 kcal/mol, which like complexes **1** and **2** exhibits a significantly greater proton affinity than the N_2 and pendant amine sites. However, the proton affinity of the distal nitrogen atom of the N_2 ligand (−2.7 kcal/mol) is predicted to be an equivalent proton acceptor to that of the diphenyl amine groups on the ligand, which have a proton affinity of −2.2 kcal/mol. Thus, the steric bulk of the pendant amine group could be influential in dictating the kinetically preferred site of the first protonation event at the N_2 ligand. Geometry-optimized models of **3** show that the sterically encumbering diphenyl amine groups favor a geometry that positions the amine away from the metal center. This structural influence, which increases the distance of the amine from the metal center, is expected to impede the movement of protons to the metal via intramolecular proton transfer. Computational analysis suggests that complexes containing a protonated pendant amine that exhibited metal protonation (complexes **1** and **2**) displayed through-space distances from the amine proton to the Mo center of less than 3.5 Å, while complexes **3** and **4**, which did not exhibit metal protonation, displayed through-space distances from the amine proton to the Mo center greater than 3.5 Å.

Further computational results predict upon protonation of the N_2 ligand the dissociation of the opposing trans N_2 ligand in complex **3** became thermodynamically favorable by 7 kcal/mol. This N_2 ligand-dissociation step increased the basicity of the protonated nitrogen atom of the diazenido (Mo−NN−H) ligand fragment by 19 kcal/mol. Furthermore, binding of an OTf^- anion in the open coordination site, trans to the diazenido group, further increased the basicity of the latter by 15 kcal/mol, significantly favoring the addition of a second equivalent of HOTf to the diazenido ligand to form the hydrazido complex $[\mathbf{3}(\mathbf{NNH_2})]^+$. These computational results echo previous kinetic studies for hydrazido formation reported by Henderson.[23] The dramatic changes in proton affinity, predicted by computational analysis, of the protonated N atom of the diazenido ligand upon dissociation of the opposing trans N_2 ligand and binding of the triflate anion to the vacant site, are consistent with the experimental observations where the addition of 1 equiv of acid to **3** results in the rapid formation of half an equivalent of the doubly protonated hydrazido ligand in $[\mathbf{3}(\mathbf{NNH_2})]^+$, precluding the observation of a monoprotonated diazenido species.

The diisopropyl groups on the pendant amine in **4** exhibit the highest proton affinity value of the series at 13.9 kcal/mol,

DOI: 10.1021/acs.inorgchem.5b00209
Inorg. Chem. XXXX, XXX, XXX−XXX

while the metal center remains the thermodynamically preferred protonation site with a proton affinity of 18 kcal/mol. The metal center is ∼14 kcal/mol more basic than the dinitrogen ligand with a proton affinity value of −1.2 kcal/mol. The dramatically higher proton affinity of the pendant amine sites versus the N_2 ligand is consistent with the predominant product observed experimentally upon treatment of **4** with HOTf containing a proton located on the pendant amine $[\mathbf{4(PP^N(H))}]^+$. The steric bulk of the diisopropyl amine groups undoubtedly preclude intramolecular proton transfer to the thermodynamically preferred metal center, as no Mo−H products were observed in ^{1}H NMR or in situ IR experiments.

CONCLUSIONS

In this study, we demonstrate that modulating the steric and electronic properties of pendant amine groups in the second coordination sphere of *trans*-$[Mo(N_2)_2(PMePh_2)_2(P^{Et}P^{NRR'})]$ complexes dramatically affects the identity of the protonated products from reactions with HOTf. In the case of **1** and **2**, less sterically encumbering pendant amine groups (i.e., NHR; R = phenyl and 2,4-difluorophenyl, respectively) promoted the formation of seven-coordinate Mo hydride complexes, presumably by facilitating intramolecular proton transfer to the metal center. Additional acid equivalents resulted in the subsequent protonation of the pendant amine sites of the seven-coordinate Mo−H complexes. The sterically encumbering and electron-deficient pendant amines in **3** resulted in exclusive protonation at the dinitrogen ligand to generate a stable Mo hydrazido complex. Reactivity of complex **5**, which did not contain a pendant amine, also proceeded to form a stable Mo hydrazido product upon treatment with HOTf. Lastly, HOTf addition to complex **4**, containing sterically encumbering and electron-rich pendant amines did not form a Mo−H, rather, protonation occurred predominately at a pendant amine site with only a minor amount of hydrazido product formation. Structural and computational analyses demonstrated that the presence of increased steric bulk surrounding the pendant amine leads to an increased distance between the protonated pendant amine and the metal center, disfavoring proton transfer to the more basic metal center. From this series of complexes, it is evident that the installation of diphenyl pendant amines in **3** provides the most suitable combination of steric and electronic properties to facilitate protonation of a metal-bound N_2 ligand. Reactions employing chemical and electrochemical sources of electrons with the *trans*-$[Mo(N_2)_2(PMePh_2)_2(P^{Et}P^{NRR'})]$ systems presented here are thus a focus of future efforts to probe the role of these flexible pendant amine sites in the reduction of N_2 to ammonia.

EXPERIMENTAL SECTION

Synthetic Procedures. *General Considerations.* All manipulations were performed under an atmosphere of dinitrogen using standard Schlenk and glovebox techniques. Solvents were dried by passage through activated alumina in an Innovative Technology, Inc., PureSolv solvent purification system. Isotopically labeled $^{15}N_2$ gas was purchased and used as received from Cambridge Isotope Laboratories. THF-d_8 and CD_2Cl_2 (Cambridge Isotope Laboratories) were dried over NaK and vacuum-transferred prior to use. Celite 405 (Fisher Scientific) was dried under vacuum for 24 h above 250 °C and stored in the glovebox prior to use. KBr (Fourier transform infrared (FTIR) grade from Aldrich) was dried under vacuum for 24 h at a temperature above 250 °C and stored in the glovebox prior to use. *trans*-$[Mo(N_2)_2(PMePh_2)_4]$ was prepared according to literature procedures.[15] Aniline and diisopropylamine were dried over CaH_2 and purified by distillation. All other reagents were purchased from commercial sources and used as received.

Solution ^{1}H, ^{19}F, ^{13}C{^{1}H}, ^{31}P{^{1}H}, and ^{15}N{^{1}H} NMR spectra were recorded on a Varian Inova or NMR S 500 MHz spectrometer. ^{1}H and ^{13}C{^{1}H} chemical shifts were referenced to residual protio impurity in deuterated solvent. ^{19}F chemical shifts were externally referenced to α,α,α-trifluorotoluene in C_6D_6 (δ = −63.72). ^{31}P{^{1}H} chemical shifts were externally referenced to 85% H_3PO_4 (δ = 0). In situ IR experiments were recorded on a Mettler-Toledo ReactIR 15 FTIR spectrometer equipped with an MCT detector, connected to a 1.5 m AgX Fiber DST series (9.5 mm × 203 mm) probe with a silicon sensor. Experiments were performed in a 5 mL two-neck pear-shaped flask under a dinitrogen atmosphere using Schlenk line techniques. IR spectra were collected in intervals of 15 s in the normal collection mode. ^{15}N{^{1}H} chemical shifts were externally referenced to neat $CH_3{}^{15}NO_2$ (δ = 0). Infrared spectra were recorded on a Thermo Scientific Nicolet iS10 FTIR spectrometer at ambient temperature and under a purge stream of dinitrogen gas. Solid-state FTIR samples were prepared as KBr pellets. Elemental analysis was performed by Atlantic Microlabs, Norcross, GA.

Diethyl (2-(Diethylphosphino)ethyl)phosphonate ($Et_2PCH_2CH_2P(O)(OEt)_2$). A stirred mixture of diethyl vinylphosphonate (7.8 mL, 0.050 mol), diethylphosphine (5.00 g, 0.055 mol, 1.1 equiv), and AIBN (0.083 g, 1 mol %) was heated at 65 °C under N_2 for 18 h. Afterward, vacuum was applied to the heated mixture for 2 h to remove volatile materials. The colorless oil was cooled to room temperature and filtered through a syringe filter. Yield: 12.34 g, 0.049 mol, 98%. ^{1}H NMR (500 MHz, CD_2Cl_2, 25 °C): δ 4.04 (m, 4H, $P(O)(OCH_2CH_3)_2$), 1.74 (m, 2H, $PCH_2CH_2PEt_2$), 1.58 (m, 2H, $PCH_2CH_2PEt_2$), 1.40 (qd, 4H, J = 8, 2.5 Hz, CH_2 (PEt_2)), 1.30 (t, 6H, J = 7 Hz, $OP(OCH_2CH_3)_2$), 1.04 (dt, 6H, J = 14, 8 Hz, CH_3 (PEt_2)). ^{31}P{^{1}H} NMR (202 MHz, CD_2Cl_2, 25 °C): δ 31.9 (d, 1P, J = 49.7 Hz, $P(O)(OCH_2CH_3)_2$), −18.0 (d, 1P, J = 49.7 Hz, PEt_2). ^{13}C{^{1}H} NMR (125 MHz, CD_2Cl_2, 25 °C): δ 61.9 (d, J = 6.6 Hz, $P(O)(OCH_2CH_3)_2$), 22.2 (dd, J = 139.2, 13.9 Hz, $PCH_2CH_2PEt_2$), 18.8 (d, J = 12.4 Hz, CH_2 (PEt_2)), 18.3 (dd, J = 16.8, 6.6 Hz, $PCH_2CH_2PEt_2$), 16.7 (d, J = 5.9 Hz, $OP(OCH_2CH_3)_2$), 9.6 (d, J = 12.8 Hz, CH_3 (PEt_2)). Anal. Calcd for $C_{10}H_{24}O_3P_2$: C, 47.24; H, 9.52. Found: C, 46.94; H, 9.45%.

Diethyl (2-phosphinoethyl)phosphine ($Et_2PCH_2CH_2PH_2$). A stirred suspension of $LiAlH_4$ (2.24 g, 0.059 mol, 1.5 equiv) in THF (100 mL) was cooled to −78 °C under an N_2 atmosphere, and then Me_3SiCl (7.5 mL, 0.059 mol, 1.5 equiv) was added via syringe. The mixture was left stirring for 30 min, after which a solution of diethyl (2-(diethylphosphino)ethyl)phosphonate (10.00 g, 0.039 mol, 1 equiv) in THF (100 mL) was added dropwise via cannula. Following the addition, the reaction mixture was left to warm to room temperature and stirred for 18 h. After this period, the reaction mixture was cooled to 0 °C and quenched by sequentially adding degassed H_2O (2 mL), a degassed aqueous solution of 15% w/w NaOH (2 mL), and an additional 6 mL of degassed H_2O via syringe. The mixture was then stirred over $MgSO_4$, and the solids were filtered and rinsed with 100 mL of Et_2O. The solvent was removed under reduced pressure to afford a colorless oil, which was filtered through a syringe filter. Yield: 3.93 g, 0.026 mol, 67%. ^{1}H NMR (500 MHz, CD_2Cl_2, 25 °C): δ 2.80 (dm, 2H, J_{PH} = 194 Hz, H_2P), 1.60−1.57 (m, 4H, PCH_2H_2P), 1.41−1.36 (m, 4H, CH_2 (PEt_2)), 1.04 (dt, 6H, J = 14, 8 Hz, CH_3 (PEt_2)). ^{31}P{^{1}H} NMR (202 MHz, CD_2Cl_2, 25 °C): δ −19.7 (d, 1P, J = 14.3 Hz, PEt_2), −128.2 (d, 1P, J = 14.5 Hz, H_2P). ^{13}C{^{1}H} NMR (125 MHz, CD_2Cl_2, 25 °C): δ 30.2 (dd, J = 15.9, 2.7 Hz, $H_2PCH_2CH_2PEt_2$), 19.0 (d, J = 12.6 Hz, CH_2 (PEt_2)), 10.6 (dd, J = 14.2, 8.4 Hz, $H_2PCH_2CH_2PEt_2$), 9.8 (d, J = 12.7 Hz, CH_3 (PEt_2)). Anal. Calcd for $C_6H_{16}P_2$: C, 48.00; H, 10.74. Found: C, 47.70; H, 10.54%.

$P^{Et}P^{NH(Ph)}$. A stirred mixture of diethyl(2-phosphinoethyl)phosphine (1.00 g, 6.66 mmol), paraformaldehyde (0.400 g, 13.3 mmol, 2.0 equiv), and aniline (1.21 mL, 13.3 mmol, 2.0 equiv) was heated at 80 °C under N_2 for 48 h. Afterward, vacuum was applied to the heated mixture for 1 h to remove volatile materials. The resulting colorless oil

DOI: 10.1021/acs.inorgchem.5b00209
Inorg. Chem. XXXX, XXX, XXX−XXX

was cooled to room temperature, stirred over $MgSO_4$ in Et_2O, filtered through a syringe filter, and the solvent was removed under reduced pressure. Yield: 2.23 g, 6.19 mmol, 93%. ^{1}H NMR (500 MHz, CD_2Cl_2, 25 °C): δ 7.17−7.14 (m, 4H, *m-H* (NPh)), 6.71−6.65 (m, 6H, *o-H* and *p-H* (NPh)), 3.97 (s, 2H, *H*NPh), 3.45−3.40 (m, 4H, PCH_2N), 1.72−1.67 (m, 2H, PCH_2CH_2PEt$_2$), 1.59−1.54 (m, 2H, PCH$_2$CH_2PEt$_2$), 1.41 (q, 4H, J = 7 Hz, CH_2 (PEt$_2$)), 1.04 (dt, 6H, J = 14, 7 Hz, CH_3 (PEt$_2$)). ^{31}P{^{1}H} NMR (202 MHz, CD_2Cl_2, 25 °C): δ −18.0 (d, 1P, J = 24 Hz, $P^{Et}P^{NH(Ph)}$), −27.2 (d, 1P, J = 24 Hz, $P^{Et}P^{NH(Ph)}$). ^{13}C{^{1}H} NMR (125 MHz, CD_2Cl_2, 25 °C): δ 149.0 (d, J = 5.5 Hz, NC_{ipso}), 129.5, 118.1, 113.5, 42.4 (d, J = 12.4 Hz, NCH_2P), 22.6 (dd, J = 15.9, 13.0 Hz, PCH$_2$CH$_2$PEt$_2$), 20.5 (t, J = 14.0 Hz, PCH$_2$CH$_2$PEt$_2$), 19.0 (d, J = 12.3 Hz, CH_2 (PEt$_2$)), 9.7 (d, J = 12.5 Hz, CH_3 (PEt$_2$)). Anal. Calcd for $C_{20}H_{30}N_2P_2$: C, 66.65; H, 8.39; N, 7.77. Found: C, 66.58; H, 8.32; N, 7.67%.

$P^{Et}P^{NH(ArF2)}$. A stirred mixture of diethyl(2-phosphinoethyl)-phosphine (1.00 g, 6.66 mmol), paraformaldehyde (0.400 g, 13.3 mmol, 2.0 equiv), and 2,4-difluoroaniline (1.36 mL, 13.3 mmol, 2.0 equiv) was heated at 80 °C under N_2 for 48 h. Afterward, vacuum was applied to the heated mixture for 1 h to remove volatile materials. The resulting colorless oil was cooled to room temperature, stirred over $MgSO_4$ in Et_2O, filtered through a syringe filter, and the solvent was removed under reduced pressure. Yield: 2.69 g, 6.22 mmol, 93%. ^{1}H NMR (500 MHz, CD_2Cl_2, 25 °C): δ 6.80−6.71 (m, 6H, *H*-ArF2), 4.03 (br s, 2H, *H*NArF2), 3.48−3.39 (m, 4H, PCH_2N), 1.73−1.69 (m, 2H, PCH_2CH$_2$PEt$_2$), 1.58−1.53 (m, 2H, PCH$_2$CH_2PEt$_2$), 1.41 (q, 4H, J = 8 Hz, CH_2 (PEt$_2$)), 1.04 (dt, 6H, J = 14, 7 Hz, CH_3 (PEt$_2$)). ^{31}P{^{1}H} NMR (202 MHz, CD_2Cl_2, 25 °C): δ −18.1 (d, 1P, J = 24.9 Hz, $P^{Et}P^{NH(ArF2)}$), −27.9 (d, 1P, J = 24.9 Hz, $P^{Et}P^{NH(ArF2)}$). ^{13}C{^{1}H} NMR (125 MHz, CD_2Cl_2, 25 °C): δ 154.9 (dd, J = 237.4, 11.2 Hz, *C*−F), 151.9 (dd, J = 241.6, 11.7 Hz, *C*−F), 134.0−133.9 (m, ArF2), 110.9 (dd, J = 21.8, 3.6 Hz, ArF2), 103.7 (dd, J = 26.9, 22.9 Hz, ArF2), 42.3 (d, J = 13.8 Hz, NCH_2P), 22.6 (dd, J = 16.1, 13.1 Hz, PCH$_2$CH$_2$PEt$_2$), 20.2 (t, J = 14.0 Hz, PCH$_2$CH$_2$PEt$_2$), 19.0 (d, J = 12.5 Hz, CH_2 (PEt$_2$)), 9.7 (d, J = 12.3 Hz, CH_3 (PEt$_2$)). ^{19}F NMR (470 MHz, THF-d_8, 25 °C): δ −127.6 (m, 1F, *p-F*), −133.7 (m, 1F, *o-F*). Anal. Calcd for $C_{20}H_{26}F_4N_2P_2$: C, 55.56; H, 6.06; N, 6.48. Found: C, 54.81; H, 6.56; N, 5.75%.

$P^{Et}P^{N(Ph)2}$. A stirred mixture of diethyl(2-phosphinoethyl)phosphine (1.00 g, 6.66 mmol), paraformaldehyde (0.400 g, 13.3 mmol, 2.0 equiv), and diphenylamine (2.25 g, 13.3 mmol, 2.0 equiv) in 2 mL of EtOH was heated at 80 °C under N_2 for 21 d. Afterward, vacuum was applied to the heated mixture for 1 h to remove volatile materials. The resulting colorless oil was cooled to room temperature and triturated in pentane to afford a white residue, which was subsequently heated in a 1:1 MeCN/EtOH solution (10 mL total). White crystals formed as the solution slowly cooled to room temperature. Storage of this solution at −35 °C overnight produced additional crystals, which were isolated by filtration and dried under vacuum. The product was recrystallized from a solution of CH_2Cl_2 (5 mL) layered with EtOH (10 mL) at −35 °C. The resulting crystals were filtered, washed with pentane, and dried under vacuum. Yield: 1.01 g, 1.97 mmol, 30%. ^{1}H NMR (500 MHz, CD_2Cl_2, 25 °C): δ 7.28−7.21 (m, 8H, *m-H* (NPh)), 7.03−6.99 (m, 8H, *o-H* (NPh)), 6.97−6.94 (m, 4H, *p-H* (NPh)), 3.95 (m, 4H, PCH_2N), 1.42−1.34 (m, 2H, PCH_2CH$_2$PEt$_2$), 1.33−1.25 (m, 2H, PCH$_2$CH_2PEt$_2$), 1.25−1.16 (m, 4H, CH_2 (PEt$_2$)), 0.94 (dt, 6H, J = 14, 8 Hz, CH_3 (PEt$_2$)). ^{31}P{^{1}H} NMR (202 MHz, CD_2Cl_2, 25 °C): δ −17.2 (d, 1P, J = 19.6 Hz, $P^{Et}P^{N(Ph)2}$), −29.4 (d, 1P, J = 19.7 Hz, $P^{Et}P^{N(Ph)2}$). ^{13}C{^{1}H} NMR (125 MHz, CD_2Cl_2, 25 °C): δ 148.8, 129.6, 122.1, 121.9 (d, J = 2.4 Hz, NC_{ipso}), 53.3 (d, J = 15.5 Hz, NCH_2P), 22.5 (t, J = 18.6 Hz, PCH$_2$CH$_2$PEt$_2$), 22.4 (t, J = 18.4 Hz, PCH$_2$CH$_2$PEt$_2$), 18.8 (d, J = 12.7 Hz, CH_2 (PEt$_2$)), 9.8 (d, J = 12.7 Hz, CH_3 (PEt$_2$)). Anal. Calcd for $C_{32}H_{38}N_2P_2$: C, 74.98; H, 7.47; N, 5.46. Found: C, 75.23; H, 7.41; N, 5.33%.

$P^{Et}P^{N(iPr)2}$. A stirred mixture of diethyl(2-phosphinoethyl)phosphine (1.00 g, 6.66 mmol) and paraformaldehyde (0.400 g, 13.3 mmol, 2.0 equiv) was heated at 80 °C under N_2 for 1 h. Diisopropylamine (1.87 mL, 13.3 mmol, 2.0 equiv) was added via syringe, and the reaction mixture was heated for 48 h. Afterward, vacuum was applied to the heated mixture for 1 h to remove volatile materials. The resulting colorless oil was cooled to room temperature, stirred over $MgSO_4$ in Et_2O, filtered through a syringe filter, and the solvent was removed under reduced pressure. Yield: 2.30 g, 6.11 mmol, 92%. ^{1}H NMR (500 MHz, CD_2Cl_2, 25 °C): δ 3.23 (sep, 4H, J = 7 Hz, NCH(CH$_3$)$_2$), 2.72−2.58 (m, 4H, PCH_2N), 1.58−1.53 (m, 2H, PCH_2CH$_2$PEt$_2$), 1.48−1.43 (m, 2H, PCH$_2$CH_2PEt$_2$), 1.38 (q, 4H, J = 8 Hz, CH_2 (PEt$_2$)), 1.04 (dt, 6H, J = 14, 7 Hz, CH_3 (PEt$_2$)), 0.98 (m, 24H, NCH(CH_3)$_2$). ^{31}P{^{1}H} NMR (202 MHz, CD_2Cl_2, 25 °C): δ −18.4 (d, 1P, J = 21 Hz, $P^{Et}P^{N(iPr)2}$), −42.6 (d, 1P, J = 21 Hz, $P^{Et}P^{N(iPr)2}$). ^{13}C{^{1}H} NMR (125 MHz, CD_2Cl_2, 25 °C): δ 48.4 (d, J = 6.8 Hz, NCH_2P), 46.5 (NCH(CH$_3$)$_2$), 46.4 (NCH(CH$_3$)$_2$), 23.4 (dd, J = 15.0, 14.2 Hz, PCH$_2$CH$_2$PEt$_2$), 23.1 (dd, J = 17.5, 11.7 Hz, PCH$_2$CH$_2$PEt$_2$), 21.1 (NCH(CH_3)$_2$), 20.4 (NCH(CH$_3$)$_2$), 19.1 (d, J = 12.7 Hz, CH_2 (PEt$_2$)), 9.9 (d, J = 12.9 Hz, CH_3 (PEt$_2$)). Anal. Calcd for $C_{20}H_{46}N_2P_2$: C, 63.80;, 12.31; N, 7.44. Found: C, 63.50; H, 12.08; N, 7.16%.

*trans-[Mo(N$_2$)$_2$(PMePh$_2$)$_2$($P^{Et}P^{NH(Ph)}$)] (**1**)*. To a stirred solution of *trans*-[Mo(N$_2$)$_2$(PMePh$_2$)$_4$] (0.500 g, 0.525 mmol) in THF (10 mL) was added a solution of $P^{Et}P^{NH(Ph)}$ (0.227 g, 0.630 mmol, 1.2 equiv) in THF (5 mL). The reaction mixture was stirred for 30 min, and then solvents were removed under reduced pressure to afford a red oil. The oil was stirred in an Et_2O suspension of CuCl (0.026 g, 0.262 mmol, 0.5 equiv) for 5 min to coordinate free phosphines, then eluted with Et_2O through a pad of neutral alumina. The product was collected as a bright orange fraction and evaporated to dryness under reduced pressure. The orange solids were dissolved in THF, and the resulting solution was layered with EtOH then stored at −35 °C overnight to produce orange crystals, which were isolated by filtration, washed with EtOH and then pentane, and dried under vacuum. Yield: 0.263 g, 0.288 mmol, 55%. Orange crystals suitable for X-ray diffraction were grown by vapor diffusion of EtOH into a THF solution of **1** at room temperature. ^{1}H NMR (500 MHz, THF-d_8, 25 °C): δ 7.41 (m, 8H, *H*-Ph (PCH$_3$Ph$_2$)), 7.19 (m, 6H, *H*-Ph (PCH$_3$Ph$_2$)), 7.12 (m, 6H, *H*-Ph (PCH$_3$Ph$_2$)), 7.02 (t, 4H, J = 8 Hz, *m-H* (NPh)), 6.55 (t, 2H, J = 7 Hz, *p-H* (NPh)), 6.43 (d, 4H, J = 9 Hz, *o-H* (NPh)), 4.48 (br s, 2H, *H*NPh), 3.16 (d, 4H, J = 6 Hz, PCH_2N), 1.91 (d, 3H, J = 5 Hz, PCH_3Ph$_2$), 1.85 (d, 3H, J = 5 Hz, PCH_3Ph$_2$), 1.76−1.65 (m, 2H, PCH_2CH$_2$PEt$_2$), 1.50−1.42 (m, 2H, PCH$_2$CH_2PEt$_2$), 1.40−1.26 (m, 4H, CH_2 (PEt$_2$)), 0.88 (dt, 6H, J = 13, 8 Hz, CH_3 (PEt$_2$)). ^{31}P{^{1}H} NMR (202 MHz, THF-d_8, 25 °C): δ 60.8 (ddd, 1P, J = 105.0, 11.9, 3.2 Hz, $P^{Et}P^{NH(Ph)}$), 50.9 (ddd, 1P, J = 103.0, 14.1, 3.2 Hz, $P^{Et}P^{NH(Ph)}$), 20.6 (ddd, 1P, J = 103.0, 15.4, 12.7 Hz, *P*CH$_3$Ph$_2$), 19.7 (dt, 1P, J = 105.0, 14.1 Hz, *P*CH$_3$Ph$_2$). IR (KBr): ν_{NH} 3401 (w), ν_{NH} 3368 (w), ν_{NN} (sym) 2003 (w), ν_{NN} (asym) 1930 (s) cm^{-1}. Anal. Calcd for $C_{46}H_{56}MoN_6P_4{\cdot}C_4H_8O$: C, 60.97; H, 6.54; N, 8.53. Found: C, 61.10; H, 6.55; N, 8.49%.

*trans-[Mo(N$_2$)$_2$(PMePh$_2$)$_2$($P^{Et}P^{NH(ArF2)}$)] (**2**)*. To a stirred solution of *trans*-[Mo(N$_2$)$_2$(PMePh$_2$)$_4$] (0.500 g, 0.525 mmol) in 4:1 Et_2O/THF (10 mL total) was added a solution of $P^{Et}P^{NH(ArF)}$ (0.272 g, 0.630 mmol, 1.2 equiv) in Et_2O (5 mL). The reaction mixture was stirred for 30 min and then solvents were removed under reduced pressure to afford a red oil. The oil was stirred in an Et_2O suspension of CuCl (0.026 g, 0.262 mmol, 0.5 equiv) for 5 min to coordinate free phosphines, then the reaction was eluted with Et_2O through a pad of neutral alumina. The product was collected as a bright orange fraction and evaporated to dryness under reduced pressure. The resulting residue was dissolved in (Me$_3$Si)$_2$O/THF, layered with EtOH, and stored at −35 °C overnight to produce orange crystals, which were isolated by filtration, washed with EtOH then pentane, and dried under vacuum. Yield: 0.247 g, 0.251 mmol, 48%. Orange crystals suitable for X-ray diffraction were grown by vapor diffusion of EtOH into a THF solution of **2** at room temperature. ^{1}H NMR (500 MHz, THF-d_8, 25 °C): δ 7.43 (m, 8H, *H*-Ph (PCH$_3$Ph$_2$)), 7.19 (m, 6H, *H*-Ph (PCH$_3$Ph$_2$)), 7.16 (m, 6H, *H*-Ph (PCH$_3$Ph$_2$)), 6.81 (ddd, 2H, J = 11, 9, 2 Hz, *H*-Ar^F), 6.71 (m, 2H, *H*-Ar^F), 6.37 (ddd, 2H, J = 9, 9, 2 Hz, *H*-Ar^F), 4.49 (br s, 2H, *H*NAr^F), 3.23 (dt, 2H, J = 14, 5 Hz, PCH_2N), 3.10 (ddd, 2H, J = 14, 7, 3 Hz, PCH_2N), 1.91 (d, 3H, J = 4 Hz, PCH_3Ph$_2$), 1.87 (d, 3H, J = 4 Hz, PCH_3Ph$_2$), 1.79−1.69 (m, 2H, PCH_2CH$_2$PEt$_2$), 1.52−1.43 (m, 2H, PCH$_2$CH_2PEt$_2$), 1.40−1.25 (m, 4H, CH_2 (PEt$_2$)), 0.88 (dt, 6H, J = 13, 8 Hz, CH_3 (PEt$_2$)). ^{31}P{^{1}H} NMR (202 MHz, THF-d_8, 25 °C): δ 61.5 (ddd, 1P, J = 107.2, 12.3, 3.7

DOI: 10.1021/acs.inorgchem.5b00209
Inorg. Chem. XXXX, XXX, XXX−XXX

Hz, $P^{Et}P^{NH(ArF)}$), 50.8 (ddd, 1P, J = 102.9, 14.1, 3.1 Hz, $P^{Et}P^{NH(ArF)}$), 20.1 (ddd, 1P, J = 103.8, 16.0, 12.6 Hz, PCH_3Ph_2), 19.3 (dt, 1P, J = 107.1, 15.3 Hz, PCH_3Ph_2). ^{19}F NMR (470 MHz, THF-d_8, 25 °C): δ −128.5 (dt, 1F, J = 9, 6 Hz, *p-F*), −133.1 (t, 1F, J = 11 Hz, *o-F*). IR (KBr): ν_{NH} 3396 (m), ν_{NH} 3322 (w), ν_{NN} (sym) 2003 (w), ν_{NN} (asym) 1939 (s) cm^{-1}. Anal. Calcd for $C_{46}H_{52}F_4MoN_6P_4{\cdot}C_4H_8O$: C, 56.82; H, 5.72; N, 7.95. Found: C, 57.21; H, 5.64; N, 7.94%.

*trans-[Mo(N$_2$)$_2$(PMePh$_2$)$_2$($P^{Et}P^{N(Ph)2}$)] (**3**).* To a stirred solution of *trans*-[Mo(N$_2$)$_2$(PMePh$_2$)$_4$] (0.500 g, 0.525 mmol) in THF (10 mL) was added a solution of $P^{Et}P^{N(Ph)2}$ (0.323 g, 0.630 mmol, 1.2 equiv) in THF (5 mL). The reaction mixture was stirred for 30 min, and then solvent was removed under reduced pressure to afford a red oil. The oil was eluted with 2:1 toluene/THF through a pad of neutral alumina, and the product was collected as a bright orange fraction, which was evaporated to dryness under reduced pressure. The resulting orange solids were washed with hexane and dried under vacuum. The solids were dissolved in THF, layered with EtOH, and stored at −35 °C overnight to afford orange crystals, which were isolated by filtration, washed with EtOH and then pentane, and dried under vacuum. Yield: 0.458 g, 0.430 mmol, 82%. Orange crystals suitable for X-ray diffraction were grown by vapor diffusion of pentane into a THF solution of **3** at room temperature. ^{1}H NMR (500 MHz, THF-d_8, 25 °C): δ 7.49 (m, 4H, *H*-Ph (PCH_3Ph_2)), 7.40 (m, 4H, *H*-Ph (PCH_3Ph_2)), 7.23 (m, 6H, *H*-Ph (PCH_3Ph_2)), 7.16 (m, 6H, *H*-Ph (PCH_3Ph_2)), 7.08 (m, 8 H, *m-H* (NPh_2)), 6.84 (t, 4H, J = 8 Hz, *p-H* (NPh_2)), 6.75 (d, 8H, J = 8 Hz, *o-H* (NPh_2)), 4.25 (dd, 2H, J = 12.5, 16 Hz, PCH_2N), 3.87 (d, 2H, J = 16.5 Hz, PCH_2N), 1.89 (d, 3H, J = 7.5 Hz, PCH_3Ph_2), 1.88 (d, 3H, J = 7.5 Hz, PCH_3Ph_2), 1.45−1.36 (m, 2H, $PCH_2CH_2PEt_2$), 1.22−1.08 (m, 4H, CH_2 (PEt_2)), 0.97−0.88 (m, 2H, $PCH_2CH_2PEt_2$), 0.68 (dt, 6H, J = 13, 7.5 Hz, CH_3 (PEt_2)). ^{31}P{^{1}H} NMR (202 MHz, THF-d_8, 25 °C): δ 77.0 (dd, 1P, J = 105.2, 13.8 Hz, $P^{Et}P^{N(Ph)2}$), 49.0 (dd, 1P, J = 104.6, 14.9 Hz, $P^{Et}P^{N(Ph)2}$), 20.1 (dt, 1P, J = 104.6, 14.5 Hz, PCH_3Ph_2), 19.7 (dt, 1P, J = 105.6, 14.5 Hz, PCH_3Ph_2). IR (KBr): ν_{NN} (sym) 2008 (w), ν_{NN} (asym) 1941 (s) cm^{-1}. Anal. Calcd for $C_{58}H_{64}MoN_6P_4$: C, 65.41; H, 6.06; N, 7.89. Found: C, 65.66; H, 6.15; N, 7.75%.

*trans-[Mo(N$_2$)$_2$(PMePh$_2$)$_2$($P^{Et}P^{N(iPr)2}$)] (**4**).* To a stirred solution of *trans*-[Mo(N$_2$)$_2$(PMePh$_2$)$_4$] (0.500 g, 0.525 mmol) in 4:1 Et_2O/THF (10 mL total) was added a solution of $P^{Et}P^{N(iPr)2}$ (0.237 g, 0.630 mmol, 1.2 equiv) in 5 mL of Et_2O. The reaction mixture was stirred for 30 min, and then solvents were removed under reduced pressure to afford a red oil. The oil was stirred in an Et_2O suspension of CuCl (0.026 g, 0.262 mmol, 0.5 equiv) for 5 min to coordinate free phosphines, then eluted with Et_2O through a pad of neutral alumina. The product was collected as a bright orange fraction and evaporated to dryness under reduced pressure. Dissolution of the resulting residue in $(Me_3Si)_2O$/pentane, followed by storage at room temperature, afforded red-orange crystals within 1 h. The crystals were isolated by filtration, washed with pentane, and dried under vacuum. Yield: 0.192 g, 0.207 mmol, 39%. Orange crystals suitable for X-ray diffraction were grown by vapor diffusion of EtOH into a THF solution of **4** at room temperature. ^{1}H NMR (500 MHz, THF-d_8, 25 °C): δ 7.39 (m, 8H, *H*-Ph (PCH_3Ph_2)), 7.15 (m, 12H, *H*-Ph (PCH_3Ph_2)), 3.00 (sep, 4H, J = 7 Hz, $NCH(CH_3)_2$), 2.90 (dd, 2H, J = 14, 13 Hz, PCH_2N), 2.53 (dd, 2H, J = 15, 4 Hz, PCH_2N), 1.84 (d, 3H, J = 4 Hz, PCH_3Ph_2), 1.77 (d, 3H, J = 4 Hz, PCH_3Ph_2), 1.69−1.61 (m, 2H, $PCH_2CH_2PEt_2$), 1.59−1.51 (m, 2H, $PCH_2CH_2PEt_2$), 1.34−1.22 (m, 4H, CH_2 (PEt_2)), 0.94 (m, 24H, $NCH(CH_3)_2$), 0.86 (dt, 6H, J = 12, 8 Hz, CH_3 (PEt_2)). ^{31}P{^{1}H} NMR (202 MHz, THF-d_8, 25 °C): δ 50.7 (ddd, 1P, J = 103.8, 13.8, 3.9 Hz, $P^{Et}P^{N(iPr)2}$), 49.3 (ddd, 1P, J = 105.8, 14.0, 2.3 Hz, $P^{Et}P^{N(iPr)2}$), 21.2 (ddd, 1P, J = 103.7, 15.3, 13.0 Hz, PCH_3Ph_2), 20.9 (ddd, 1P, J = 106.4, 16.5, 13.0 Hz, PCH_3Ph_2). IR (KBr): ν_{NN} (sym) 2000 (w), ν_{NN} (asym) 1930 (s) cm^{-1}. Anal. Calcd for $C_{46}H_{72}MoN_6P_4$: C, 59.47; H, 7.81; N, 9.05. Found: C, 59.67; H, 7.90; N, 9.12%.

*trans-[Mo(N$_2$)$_2$(PMePh$_2$)$_2$(depe)] (**5**).* To a stirred solution of *trans*-[Mo(N$_2$)$_2$(PMePh$_2$)$_4$] (0.200 g, 0.210 mmol) in THF (5 mL) was added depe (54 μL, 0.231 mmol, 1.1 equiv). The reaction mixture was stirred for 30 min, and then solvents were removed under reduced pressure. Dissolution of the resulting red oil in $(Me_3Si)_2O$/hexane, followed by storage at room temperature overnight, afforded red-orange crystals. The crystals were isolated by filtration, washed with pentane, and dried under vacuum. Yield: 0.119 g, 0.157 mmol, 75%. ^{1}H NMR (500 MHz, THF-d_8, 25 °C): δ 7.39 (m, 8H, *H*-Ph (PCH_3Ph_2)), 7.15 (m, 12H, *H*-Ph (PCH_3Ph_2)), 1.83 (d, 6H, J = 4 Hz, PCH_3Ph_2), 1.47−1.37 (m, 4H, $PCH_2CH_2PEt_2$), 1.35−1.19 (m, 8H, CH_2 (PEt_2)), 0.86 (dt, 12H, J = 12, 8 Hz, CH_3 (PEt_2)). ^{31}P{^{1}H} NMR (202 MHz, THF-d_8, 25 °C): δ 50.2 (m, 2P, depe), 20.9 (m, 2P, PCH_3Ph_2). IR (KBr): ν_{NN} (sym) 2003 (w), ν_{NN} (asym) 1939 (s) cm^{-1}. Anal. Calcd for $C_{36}H_{50}MoN_4P_4$: C, 56.99; H, 6.64; N, 7.38. Found: C, 57.23; H, 6.65; N, 7.35%.

*Stoichiometric Protonation (NMR) of trans-[Mo(N$_2$)$_2$(PMePh$_2$)$_2$(P−P)] Complexes **1**, **2**, and **4** with HOTf.* A J. Young tube was charged with a solution of *trans*-[Mo(N$_2$)$_2$(PMePh$_2$)$_2$(P−P)] in THF-d_8 (28 mM, 0.6 mL total) and then sealed with a rubber septum. The J. Young tube was immersed in a dry ice/acetone bath for 10 min (keeping the upper portion of the tube cold as well) before HOTf (1.5 μL, 0.017 mmol, 1 equiv) was added via syringe. The NMR tube was quickly tilted several times to ensure complete mixing and then cooled in the dry ice/acetone bath for an additional 5 min. The sample was then inserted into the NMR spectrometer precooled to −40 °C. After a 10 min equilibration period, ^{1}H, ^{31}P{^{1}H}, and ^{19}F NMR spectra were acquired. This was repeated for each subsequent equivalent of HOTf that was added to the sample.

*Stoichiometric Protonation (in Situ IR) of trans-[Mo(N$_2$)$_2$(PMePh$_2$)$_2$(P−P)] Complexes **1**−**5** with HOTf.* In situ IR experiments were recorded on a Mettler-Toledo ReactIR 15 FTIR spectrometer equipped with an MCT detector, connected to a 1.5 m AgX Fiber DST series (9.5 mm × 203 mm) probe with a silicon sensor. Experiments were performed in a 5 mL two-neck pear-shaped flask equipped with a magnetic stirbar and sealed with rubber septa, under a dinitrogen atmosphere using Schlenk line techniques. Typical reactions contained 17 mM Mo complex in 1 mL of THF. The reactions were cooled in a MeCN/CO_2(s) bath (−41 °C), and then IR spectra were collected in intervals of 15 s in the normal collection mode. Stepwise addition of HOTf (1.5 μL, 0.017 mmol, 1 equiv at a time) was monitored throughout the duration of the experiments.

*trans-[Mo(H)(N$_2$)$_2$(PMePh$_2$)$_2$($P^{Et}P^{NH(Ph)}$)](OTf) (**[1H]$^+$**).* The protonation procedures described above were followed using a solution of **1** (0.018 g, 0.017 mmol) and HOTf (1.5 μL, 0.017 mmol, 1 equiv). Major isomer: ^{1}H NMR (500 MHz, THF-d_8, −40 °C): δ 7.53−7.42 (m, 14H, *H*-Ph (PCH_3Ph_2)), 7.25 (m, 6H, *H*-Ph (PCH_3Ph_2)), 7.13 (m, 6H, *H*-Ph (NPh)), 6.79 (d, 4H, J = 8 Hz, *H*-Ph (NPh)), 6.70 (t, 2H, J = 7 Hz, PCH_2N), 6.54 (d, 2H, J = 7 Hz, PCH_2N), 4.97 (br s, 2H, *H*NPh), 2.01 (d, 3H, J = 6 Hz, PCH_3Ph_2), 1.85 (d, 3H, J = 6 Hz, PCH_3Ph_2), 1.63 (m, 2H, $PCH_2CH_2PEt_2$), 1.43 (m, 2H, $PCH_2CH_2PEt_2$), 1.03 (m, 4H, CH_2 (PEt_2)), 0.87 (m, 6H, CH_3 (PEt_2)), −3.91 (m, 1H, Mo−*H*). ^{31}P{^{1}H} NMR (202 MHz, THF-d_8, −40 °C): δ 89.7 (m, 1P, $P^{Et}P^{NH(Ph)}$), 43.6 (m, 1P, $P^{Et}P^{NH(Ph)}$), 20.2 (m, 1P, PCH_3Ph_2), 6.5 (m, 1P, PCH_3Ph_2). ^{19}F NMR (470 MHz, THF-d_8, −40 °C): δ −80.2 (s, $^-$OTf). IR (THF, −40 °C): ν_{NN} (asym) 2024 (s) cm^{-1}. Minor isomer: ^{1}H NMR (500 MHz, THF-d_8, −40 °C): δ −4.29 (m, Mo−*H*). ^{31}P{^{1}H} NMR (202 MHz, THF-d_8, −40 °C): δ 75.8 (m, $P^{Et}P^{NH(Ph)}$), 50.4 (m, $P^{Et}P^{NH(Ph)}$), 20.2 (m, PCH_3Ph_2), 6.5 (m, PCH_3Ph_2).

*trans-[Mo(H)(N$_2$)$_2$(PMePh$_2$)$_2$($P^{Et}P^{NH(Ph)}$(H))](OTf)$_2$ (**[1H(PP^N(H))]$^{2+}$**).* The protonation procedures described above were followed using a solution of [**1H**]$^+$ (generated in situ) and HOTf (1.5 μL, 0.017 mmol, 1 equiv). Major isomer: ^{1}H NMR (500 MHz, THF-d_8, −40 °C): δ 8.29 (br s, 3H, *H*NPh and H_2NPh), 7.54−7.45 (m, 14H, *H*-Ph (PCH_3Ph_2)), 7.33 (t, 6H, J = 8 Hz, *H*-Ph (PCH_3Ph_2)), 7.15 (m, 2H, PCH_2N), 7.10 (m, 2H, PCH_2N), 7.02 (m, 10H, *H*-Ph (NPh)), 2.10 (d, 3H, J = 6 Hz, PCH_3Ph_2), 1.88 (d, 3H, J = 6 Hz, PCH_3Ph_2), 1.56 (m, 2H, $PCH_2CH_2PEt_2$), 1.36 (m, 2H, $PCH_2CH_2PEt_2$), 1.05 (m, 4H, CH_2 (PEt_2)), 0.94 (dt, 6H, J = 15, 8 Hz, CH_3 (PEt_2)), −4.63 (m, 1H, Mo−*H*). ^{31}P{^{1}H} NMR (202 MHz, THF-d_8, −40 °C): δ 78.4 (m, 1P, $P^{Et}P^{NH(Ph)}$), 42.1 (m, 1P, $P^{Et}P^{NH(Ph)}$), 19.7 (m, 1P, PCH_3Ph_2), 4.4 (m, 1P, PCH_3Ph_2). ^{19}F NMR (470 MHz, THF-d_8, −40 °C): δ −80.3 (s, $^-$OTf). IR (THF, −40 °C): ν_{NN} (asym) 2044 (s) cm^{-1}. Minor isomer: ^{1}H NMR (500 MHz, THF-d_8, −40 °C): δ −4.47 (m, Mo−*H*).

DOI: 10.1021/acs.inorgchem.5b00209
Inorg. Chem. XXXX, XXX, XXX−XXX

$^{31}P\{^{1}H\}$ NMR (202 MHz, THF-d_8, −40 °C): δ 80.2 (m, $P^{Et}P^{NH(Ph)}$), 45.3 (m, $P^{Et}P^{NH(Ph)}$), 20.5 (m, PCH_3Ph_2), 4.4 (m, PCH_3Ph_2).

*trans-[Mo(H)(N$_2$)$_2$(PMePh$_2$)$_2$($P^{Et}P^{NH(ArF2)}$)](OTf) ([**2H**]$^+$).* The protonation procedures described above were followed using a solution of **2** (0.018 g, 0.017 mmol) and HOTf (1.5 μL, 0.017 mmol, 1 equiv). Major isomer: ^{1}H NMR (500 MHz, THF-d_8, −40 °C): δ 7.53−7.42 (m, 12H, *H*-Ph (PCH_3Ph_2)), 7.34−7.27 (m, 8H, *H*-Ph (PCH_3Ph_2)), 7.03 (m, 2H, *H*-ArF2), 6.87 (m, 4H, *H*-ArF2), 6.15 (br s, 2H, *H*NArF2), 2.06 (m, 4H, PCH_2N), 2.01 (d, 3H, *J* = 5 Hz, PCH_3Ph_2), 1.85 (d, 3H, *J* = 5 Hz, PCH_3Ph_2), 1.62 (dd, 2H, *J* = 15, 7 Hz, $PCH_2CH_2PEt_2$), 1.53 (dd, 2H, *J* = 15, 7 Hz, $PCH_2CH_2PEt_2$), 1.03 (m, 4H, CH_2 (PEt_2)), 0.88 (dt, 6H, *J* = 14, 7 Hz, CH_3 (PEt_2)), −3.96 (m, 1H, Mo−*H*). $^{31}P\{^{1}H\}$ NMR (202 MHz, THF-d_8, −40 °C): δ 91.3 (m, 1P, $P^{Et}P^{NH(ArF2)}$), 43.5 (m, 1P, $P^{Et}P^{NH(ArF2)}$), 20.2 (m, 1P, PCH_3Ph_2), 6.2 (m, 1P, PCH_3Ph_2). ^{19}F NMR (470 MHz, THF-d_8, −40 °C): δ −80.2 (s, 3F, $^{-}$OTf), −127.6 (s, 2F, Ar-*F*), −132.3 (s, 2F, Ar-*F*). IR (THF, −40 °C): ν_{NN} (asym) 2024 (s) cm^{-1}. Minor isomer: ^{1}H NMR (500 MHz, THF-d_8, −40 °C): δ −4.20 (m, 0.2H, Mo−*H*). $^{31}P\{^{1}H\}$ NMR (202 MHz, THF-d_8, −40 °C): δ 75.6 (m, $P^{Et}P^{NH(ArF2)}$), 53.2 (m, $P^{Et}P^{NH(ArF2)}$), 20.2 (m, PCH_3Ph_2), 6.2 (m, PCH_3Ph_2). ^{19}F NMR (470 MHz, THF-d_8, −40 °C): δ −80.2 (s, $^{-}$OTf), −126.7 (s, Ar-*F*), −130.6 (s, Ar-*F*).

*trans-[Mo(H)(N$_2$)$_2$(PMePh$_2$)$_2$($P^{Et}P^{NH(ArF2)}$(H))](OTf)$_2$ ([**2H-(PP^N(H))**]$^{2+}$).* The protonation procedures described above were followed using a solution of [**2H**]$^+$ (generated in situ) and HOTf (1.5 μL, 0.017 mmol, 1 equiv). Major isomer: ^{1}H NMR (500 MHz, THF-d_8, −40 °C): δ 7.52−7.43 (m, 12H, *H*-Ph (PCH_3Ph_2)), 7.34−7.27 (m, 8H, *H*-Ph (PCH_3Ph_2)), 7.16 (m, 4H, *H*-ArF2), 6.99 (m, 2H, *H*-ArF2), 2.31−2.17 (m, 4H, PCH_2N), 2.05 (d, 3H, *J* = 5 Hz, PCH_3Ph_2), 1.84 (d, 3H, *J* = 6 Hz, PCH_3Ph_2), 1.60 (m, 2H, $PCH_2CH_2PEt_2$), 1.47 (m, 2H, $PCH_2CH_2PEt_2$), 1.04 (m, 4H, CH_2 (PEt_2)), 0.90 (dt, 6H, *J* = 15, 7 Hz, CH_3 (PEt_2)), −4.29 (m, 1H, Mo−*H*). The ^{1}H signal corresponding to the pendant amine N−H proton could not be identified. $^{31}P\{^{1}H\}$ NMR (202 MHz, THF-d_8, −40 °C): δ 86.4 (m, 1P, $P^{Et}P^{NH(ArF2)}$), 42.8 (m, 1P, $P^{Et}P^{NH(ArF2)}$), 20.4 (m, 1P, PCH_3Ph_2), 5.4 (m, 1P, PCH_3Ph_2). ^{19}F NMR (470 MHz, THF-d_8, −40 °C): δ −80.5 (s, $^{-}$OTf). The ^{19}F signals for the Ar-*F* nuclei were not observed. IR (THF, −40 °C): ν_{NN} (asym) 2046 (s) cm^{-1}. Minor isomer: ^{1}H NMR (500 MHz, THF-d_8, −40 °C): The signal corresponding to the Mo−H proton could not be identified since it is obscured by the resonance of the major isomer. $^{31}P\{^{1}H\}$ NMR (202 MHz, THF-d_8, −40 °C): δ 76.1 (m, $P^{Et}P^{NH(ArF2)}$), 48.3 (m, $P^{Et}P^{NH(ArF2)}$), 20.4 (m, PCH_3Ph_2), 5.4 (m, PCH_3Ph_2).

*trans-[Mo(NNH$_2$)(OTf)(PMePh$_2$)$_2$($P^{Et}P^{N(Ph)2}$)](OTf) ([**3(NNH$_2$)**]$^+$).* To a cooled (−35 °C) solution of **3** (0.250 g, 0.235 mmol) in THF (10 mL) was added HOTf (41.5 μL, 0.469 mmol, 2 equiv). The solution immediately turned red in color and was left stirring for 1 min. The solution was stored at −35 °C for 10 min and then evaporated to dryness under reduced pressure. Dissolution of the resulting residue in $(Me_3Si)_2O$/fluorobenzene, followed by storage at room temperature overnight, caused the product to precipitate as pink powder. The product was isolated by filtration, dissolved in a mixture of THF and Et_2O to remove residual fluorobenzene, and dried under vacuum. Yield: 0.130 g, 0.097 mmol, 41%. Yellow crystals suitable for X-ray diffraction were grown from a toluene/THF solution of [**3(NNH$_2$)**]$^+$ at room temperature over the course of two months. ^{1}H NMR (500 MHz, THF-d_8, 25 °C): δ 9.47 (s, 2H, Mo═N−NH_2), 7.59 (m, 2H, *H*-Ph), 7.46 (m, 6H, *H*-Ph), 7.34 (m, 10H, *H*-Ph), 7.17 (m, 10H, *H*-Ph), 6.95 (m, 4H, *H*-Ph), 6.91 (m, 4H, *H*-Ph), 6.77 (m, 4H, *H*-Ph), 4.93 (dd, 1H, *J* = 16, 10 Hz, PCH_2N), 4.40 (dd, 1H, *J* = 16, 13 Hz, PCH_2N), 4.12 (dd, 1H, *J* = 16, 4 Hz, PCH_2N), 3.94 (d, 1H, *J* = 16 Hz, PCH_2N), 2.14 (d, 3H, *J* = 6 Hz, PCH_3Ph_2), 1.95 (d, 3H, *J* = 6 Hz, PCH_3Ph_2), 1.67−1.56 (m, 2H, $PCH_2CH_2PEt_2$), 1.54−1.38 (m, 2H, $PCH_2CH_2PEt_2$), 1.36−1.26 (m, 2H, CH_2 (PEt_2)), 1.21−0.94 (m, 2H, CH_2 (PEt_2)), 0.84 (dt, 3H, *J* = 15, 8 Hz, CH_3 (PEt_2)), 0.62 (dt, 3H, *J* = 22, 7 Hz, CH_3 (PEt_2)). $^{31}P\{^{1}H\}$ NMR (202 MHz, THF-d_8, 25 °C): δ 64.1 (m, 1P, $P^{Et}P^{N(Ph)2}$), 41.2 (m, 1P, $P^{Et}P^{N(Ph)2}$), 8.4 (m, 1P, PCH_3Ph_2), 6.5 (m, 1P, PCH_3Ph_2). ^{19}F NMR (470 MHz, THF-d_8, 25 °C): δ −78.0 (s, 1F, Mo(OTf)), −80.0 (s, 1F, $^{-}$OTf). IR (KBr): ν_{NH} 3312 (m), ν_{NH} 3249 (m), ν_{NH} 3129 (m) cm^{-1}. Anal. Calcd for $C_{60}H_{66}F_6MoN_4O_6P_4S_2$: C, 53.89; H, 4.98; N, 4.19. Found: C, 54.03; H, 5.12; N, 4.17%.

*trans-[Mo(N$_2$)$_2$(PMePh$_2$)$_2$($P^{Et}P^{N(iPr)2}$(H))](OTf) ([**4(PP^N(H))**]$^+$).* The protonation procedures described above were followed using a solution of **4** (0.016 g, 0.017 mmol) and HOTf (3.0 μL, 0.034 mmol, 2 equiv). $^{31}P\{^{1}H\}$ NMR (202 MHz, THF-d_8, −40 °C): δ 50.9 (m, 1P, $P^{Et}P^{N(iPr)2}$), 47.5 (m, 1P, $P^{Et}P^{N(iPr)2}$), 23.3 (m, 1P, PCH_3Ph_2), 18.4 (m, 1P, PCH_3Ph_2). ^{19}F NMR (470 MHz, THF-d_8, −40 °C): δ −77.5 (s, OTf$^-$). IR (THF, −40 °C): ν_{NN} (asym) 1957 (s) cm^{-1}.

*trans-[Mo(NNH$_2$)(PMePh$_2$)$_2$($P^{Et}P^{N(iPr)2}$(H))](OTf)$_2$ ([**4(NNH$_2$)-(PP^N(H))**]$^{2+}$).* The protonation procedures described above were followed using a solution of [**4(PP^N(H))**]$^+$ (generated in situ) and HOTf (3.0 μL, 0.034 mmol, 2 equiv). Since a trace amount of this product was generated, it could only be detected from ^{15}N and $^{1}H-^{15}N$ HMBC experiments using the $^{15}N_2$-labeled isotopologue (see below).

*trans-[Mo(NNH$_2$)(OTf)(PMePh$_2$)$_2$(depe)](OTf) ([**5(NNH$_2$)**]$^+$).* To a cooled (−35 °C) solution of **5** (0.175 g, 0.231 mmol) in THF (10 mL) was added HOTf (41 μL, 0.461 mmol, 2 equiv). The solution immediately turned red in color and was left stirring for 1 min. The solution was stored at −35 °C for 10 min and then evaporated to dryness under reduced pressure. The resulting residue was stirred in $(Me_3Si)_2O$/fluorobenzene to afford light brown precipitate, which was isolated by filtration, washed with pentane, and dissolved in a mixture of THF and Et_2O to remove residual fluorobenzene, and dried under vacuum. Yield: 0.235 g, 0.228 mmol, 99%. ^{1}H NMR (500 MHz, THF-d_8, 25 °C): δ 9.27 (s, 2H, Mo═N−NH_2), 7.50 (m, 4H, *H*-Ph (PCH_3Ph_2)), 7.42−7.30 (m, 12H, *H*-Ph (PCH_3Ph_2)), 7.24 (t, 4H, *J* = 8 Hz, *H*-Ph (PCH_3Ph_2)), 2.10−2.02 (m, 2H, CH_2 (PEt_2)), 1.93 (d, 6H, *J* = 6 Hz, PCH_3Ph_2), 1.87−1.78 (m, 4H, CH_2 (PEt_2)), 1.40 (tt, 2H, *J* = 14.8, 7.5 Hz, $Et_2PCH_2CH_2PEt_2$), 1.24−1.16 (m, 2H, CH_2 (PEt_2)), 1.11 (tt, 2H, *J* = 14.4, 7.2 Hz, $Et_2PCH_2CH_2PEt_2$), 0.98 (dt, 12H, *J* = 7.5, 5.7 Hz, CH_3 (PEt_2)). $^{31}P\{^{1}H\}$ NMR (202 MHz, THF-d_8, 25 °C): δ 42.5 (m, 2P, depe), 9.3 (m, 2P, $PMePh_2$). ^{19}F NMR (470 MHz, THF-d_8, 25 °C): δ −78.5 (s, 1F, Mo(OTf)), −80.1 (s, 1F, $^{-}$OTf). IR (KBr): ν_{NH} 3254 (m), ν_{NH} 3102 (m) cm^{-1}. Anal. Calcd for $C_{38}H_{52}F_6MoN_2O_6P_4S_2$: C, 44.28; H, 5.08; N, 2.72. Found: C, 44.44; H, 4.89; N, 2.51%.

General Procedure for Ammonia Production Reactions. A 100 mL round-bottom single neck (14/20 outer joint) Schlenk flask equipped with a magnetic stir bar was charged with Mo complex (0.017 mmol) and solvent (2 mL) under a N_2 atmosphere. The flask was sealed with a rubber septum, and acid (30−35 equiv) was added via syringe to the stirred solution/suspension at room temperature. After 20 h, the flask was immersed in a dewar containing liquid N_2 and evacuated. An aqueous solution of 30% w/w KOH (2 mL) was added to the frozen reaction mixture, which was stirred as it warmed to room temperature and distilled under static vacuum into dilute aqueous acid solution (0.5 M, 4 mL). The resulting acid solution was analyzed for ammonia and hydrazine by the indophenol[28] and *p*-(dimethylamino)-benzaldehyde[29] methods, respectively.

Computational Details. All computational structures were optimized in Gaussian 09[30] without symmetry constraints using B3P86[31] functional and the Stuttgart basis set with effective core potential (ECP)[32] for Mo and the 6-31G** basis set[33] for all the remaining atoms. The ultrafine integration grid was employed in all calculations, to ensure the stability of the optimization procedure for the investigated molecules. Each stationary point was confirmed to be a real local minimum on the potential energy surface by the absence of imaginary frequencies in the frequency calculation at the same level of theory. The reported thermodynamic pK_a values are for THF solutions at the standard state (*T* = 298 K, *P* = 1 atm of N_2, 1 mol/L concentration of all species in THF) as modeled by a polarized continuum model[34] and are calculated relative to the value of Et_3NH^+ (pK_a = 12.5),[35] which is assigned as an experimental value to anchor the calculated pK_a scale. Bondi radii[36] were used with a scale factor (α) of 1.0.

DOI: 10.1021/acs.inorgchem.5b00209
Inorg. Chem. XXXX, XXX, XXX−XXX

■ ASSOCIATED CONTENT

Supporting Information

Figures, tables, and CIF files providing multinuclear NMR data, $^{1}H-^{15}N$ HMBC spectra, $^{31}P\{^{1}H\}$ NMR spectra, details of syntheses, results from ammonia production reactions, and crystallographic information; experimental results for ^{15}N labeling studies; coordinates for DFT optimized structures. This material is available free of charge via the Internet at http://pubs.acs.org.

■ AUTHOR INFORMATION

Corresponding Author

*E-mail: Michael.Mock@pnnl.gov.

Notes

The authors declare no competing financial interest.

■ ACKNOWLEDGMENTS

This research was supported as part of the Center for Molecular Electrocatalysis, an Energy Frontier Research Center funded by the U.S. Department of Energy, Office of Science, Office of Basic Energy Sciences. Computational resources provided by the National Energy Research Scientific Computing Center (NERSC) at Lawrence Berkeley National Laboratory. Pacific Northwest National Laboratory is operated by Battelle for the U.S. Department of Energy.

■ REFERENCES

(1) (a) Chatt, J.; Dilworth, J. R.; Richards, R. L. *Chem. Rev.* **1978**, *78*, 589−625. (b) Broda, H.; Hinrichsen, S.; Tuczek, F. *Coord. Chem. Rev.* **2013**, *257*, 587−598.

(2) Tanabe, Y.; Nishibayashi, Y. *Coord. Chem. Rev.* **2013**, *257*, 2551−2564.

(3) (a) Baumann, J. A.; George, T. A. *J. Am. Chem. Soc.* **1980**, *102*, 6153−6154. (b) Chatt, J.; Pearman, A. J.; Richards, R. L. *J. Chem. Soc., Dalton Trans.* **1977**, 1852−1860. (c) Chatt, J.; Pearman, A. J.; Richards, R. L. *Nature* **1975**, *253*, 39−40. (d) Hidai, M.; Mizobe, Y.; Takahashi, T.; Uchida, Y. *Chem. Lett.* **1978**, *7*, 1187−1188.

(4) (a) Chatt, J.; Heath, G. A.; Richards, R. L. *J. Chem. Soc., Dalton Trans.* **1974**, 2074−2082. (b) Abubakar, M.; Hughes, D. L.; Hussain, W.; Leigh, G. J.; Macdonald, C. J.; Ali, H. M. *J. Chem. Soc., Dalton Trans.* **1988**, 2545−2553. (c) Barclay, J. E.; Hills, A.; Hughes, D. L.; Leigh, G. J.; Macdonald, C. J.; Abubakar, M.; Mohdali, H. *J. Chem. Soc., Dalton Trans.* **1990**, 2503−2507.

(5) Yuki, M.; Miyake, Y.; Nishibayashi, Y.; Wakiji, I.; Hidai, M. *Organometallics* **2008**, *27*, 3947−3953.

(6) Yuki, M.; Midorikawa, T.; Miyake, Y.; Nishibayashi, Y. *Organometallics* **2009**, *28*, 4741−4746.

(7) Yuki, M.; Miyake, Y.; Nishibayashi, Y. *Organometallics* **2009**, *28*, 5821−5827.

(8) Yandulov, D. V.; Schrock, R. R. *Science* **2003**, *301*, 76−78.

(9) Reithofer, M. R.; Schrock, R. R.; Müller, P. *J. Am. Chem. Soc.* **2010**, *132*, 8349−8358.

(10) Mock, M. T.; Chen, S.; O'Hagan, M.; Rousseau, R.; Dougherty, W. G.; Kassel, W. S.; Bullock, R. M. *J. Am. Chem. Soc.* **2013**, *135*, 11493−11496.

(11) Weiss, C. J.; Egbert, J. D.; Chen, S.; Helm, M. L.; Bullock, R. M.; Mock, M. T. *Organometallics* **2014**, *33*, 2189−2200.

(12) Labios, L. A.; Weiss, C. J.; Egbert, J. D.; Lense, S.; Bullock, R. M.; Dougherty, W. G.; Kassel, W. S.; Mock, M. T. *Z. Anorg. Allg. Chem.* **2015**, *641*, 105−117.

(13) (a) Heiden, Z. M.; Chen, S.; Labios, L. A.; Bullock, R. M.; Walter, E. D.; Tyson, E. L.; Mock, M. T. *Organometallics* **2014**, *33*, 1333−1336. (b) Heiden, Z. M.; Chen, S.; Mock, M. T.; Dougherty, W. G.; Kassel, W. S.; Rousseau, R.; Bullock, R. M. *Inorg. Chem.* **2013**, *52*, 4026−4039.

(14) (a) Chatt, J.; Wedd, A. G. *J. Organomet. Chem.* **1971**, *27*, C15. (b) George, T. A.; Hayes, R. K.; Mohammed, M. Y.; Pickett, C. J. *Inorg. Chem.* **1989**, *28*, 3269−3270. (c) George, T. A.; Noble, M. E. *Inorg. Chem.* **1978**, *17*, 1678−1679. (d) George, T. A.; Seibold, C. D. *Inorg. Chem.* **1973**, *12*, 2544−2547.

(15) (a) Lazarowych, N. J.; Morris, R. H.; Ressner, J. M. *Inorg. Chem.* **1986**, *25*, 3926−3932. (b) Ning, Y.; Sarjeant, A. A.; Stern, C. L.; Peterson, T. H.; Nguyen, S. T. *Inorg. Chem.* **2012**, *51*, 3051−3058.

(16) (a) Levitre, S. A.; Tso, C. C.; Cutler, A. R. *J. Organomet. Chem.* **1986**, *308*, 253−259. (b) Sircoglou, M.; Saffon, N.; Miqueu, K.; Bouhadir, G.; Bourissou, D. *Organometallics* **2013**, *32*, 6780−6784.

(17) MacKay, B. A.; Fryzuk, M. D. *Chem. Rev.* **2004**, *104*, 385−401.

(18) Hussain, W.; Leigh, G. J.; Ali, H. M.; Pickett, C. J.; Rankin, D. A. *J. Chem. Soc., Dalton Trans.* **1984**, 1703−1708.

(19) (a) Mock, M. T.; Chen, S.; Rousseau, R.; O'Hagan, M. J.; Dougherty, W. G.; Kassel, W. S.; DuBois, D. L.; Bullock, R. M. *Chem. Commun.* **2011**, *47*, 12212−12214. (b) Weiss, C. J.; Groves, A. N.; Mock, M. T.; Dougherty, W. G.; Kassel, W. S.; Helm, M. L.; DuBois, D. L.; Bullock, R. M. *Dalton Trans.* **2012**, *41*, 4517−4529.

(20) Rowland, R. S.; Taylor, R. *J. Phys. Chem.* **1996**, *100*, 7384−7391.

(21) (a) Curtis, M. D.; Shiu, K. B. *Inorg. Chem.* **1985**, *24*, 1213−1218. (b) Baker, P. K.; Al-Jahdali, M.; Meehan, M. M. *J. Organomet. Chem.* **2002**, *648*, 99−108. (c) Baker, P. K.; Drew, M. G. B.; Moore, D. S. *J. Organomet. Chem.* **2002**, *664*, 45−58. (d) Öztopcu, Ö.; Holzhacker, C.; Puchberger, M.; Weil, M.; Mereiter, K.; Veiros, L. F.; Kirchner, K. *Organometallics* **2013**, *32*, 3042−3052.

(22) Chatt, J. *J. Organomet. Chem.* **1975**, *100*, 17−28.

(23) (a) Henderson, R. A. *J. Chem. Soc., Dalton Trans.* **1982**, 917−925. (b) Henderson, R. A. *J. Chem. Soc., Dalton Trans.* **1984**, 2259−2263.

(24) (a) Krahmer, J.; Broda, H.; Näther, C.; Peters, G.; Thimm, W.; Tuczek, F. *Eur. J. Inorg. Chem.* **2011**, *2011*, 4377−4386. (b) Anderson, S. N.; Fakley, M. E.; Richards, R. L.; Chatt, J. *J. Chem. Soc., Dalton Trans.* **1981**, 1973−1980.

(25) (a) Roemer, R.; Gradert, C.; Bannwarth, A.; Peters, G.; Naether, C.; Tuczek, F. *Dalton Trans.* **2011**, *40*, 3229−3236. (b) Chatt, J.; Pearman, A. J.; Richards, R. L. *J. Chem. Soc., Dalton Trans.* **1978**, 1766−1776. (c) Lehnert, N.; Tuczek, F. *Inorg. Chem.* **1999**, *38*, 1659−1670.

(26) Stephan, G. C.; Peters, G.; Lehnert, N.; Habeck, C. M.; Näther, C.; Tuczek, F. *Can. J. Chem.* **2005**, *83*, 385−402.

(27) (a) Heath, G. A.; Mason, R.; Thomas, K. M. *J. Am. Chem. Soc.* **1974**, *96*, 259−260. (b) Hidai, M.; Kodama, T.; Sato, M.; Harakawa, M.; Uchida, Y. *Inorg. Chem.* **1976**, *15*, 2694−2697. (c) Stephan, G.; Naether, C.; Tuczek, F. *Acta Crystallogr., Sect. E: Struct. Rep. Online* **2008**, *64*, M629−U241.

(28) (a) Chaney, A. L.; Marbach, E. P. *Clin. Chem.* **1962**, *8*, 130−132. (b) Weatherburn, M. W. *Anal. Chem.* **1967**, *39*, 971−974.

(29) Watt, G. W.; Chrisp, J. D. *Anal. Chem.* **1952**, *24*, 2006−2008.

(30) Frisch, M. J.; Trucks, G. W.; Schlegel, H. B.; Scuseria, G. E.; Robb, M. A.; Cheeseman, J. R.; Scalmani, G.; Barone, V.; Mennucci, B.; Petersson, G. A.; Nakatsuji, H.; Caricato, M.; Li, X.; Hratchian, H. P.; Izmaylov, A. F.; Bloino, J.; Zheng, G.; Sonnenberg, J. L.; Hada, M.; Ehara, M.; Toyota, K.; Fukuda, R.; Hasegawa, J.; Ishida, M.; Nakajima, T.; Honda, Y.; Kitao, O.; Nakai, H.; Vreven, T.; Montgomery, J. A., Jr.; Peralta, J. E.; Ogliaro, F.; Bearpark, M.; Heyd, J. J.; Brothers, E.; Kudin, K. N.; Staroverov, V. N.; Kobayashi, R.; Normand, J.; Raghavachari, K.; Rendell, A.; Burant, J. C.; Iyengar, S. S.; Tomasi, J.; Cossi, M.; Rega, N.; Millam, J. M.; Klene, M.; Knox, J. E.; Cross, J. B.; Bakken, V.; Adamo, C.; Jaramillo, J.; Gomperts, R.; Stratmann, R. E.; Yazyev, O.; Austin, A. J.; Cammi, R.; Pomelli, C.; Ochterski, J. W.; Martin, R. L.; Morokuma, K.; Zakrzewski, V. G.; G. A. Voth, P. S.; Dannenberg, J. J.; Dapprich, S.; Daniels, A. D.; Farkas, O.; Foresman, J. B.; Ortiz, J. V.; Cioslowski, J.; Fox, D. J. *Gaussian 09;* Gaussian, Inc.: Wallingford, CT, 2009.

(31) (a) Becke, A. D. *J. Chem. Phys.* **1993**, *98*, 5648−5652. (b) Perdew, J. P. *Phys. Rev. B* **1986**, *33*, 8822−8824.

(32) Andrae, D.; Häußermann, U.; Dolg, M.; Stoll, H.; Preuß, H. *Theor. Chem. Acc.* **1990**, *77*, 123−141.

DOI: 10.1021/acs.inorgchem.5b00209
Inorg. Chem. XXXX, XXX, XXX−XXX

(33) (a) Francl, M. M.; Pietro, W. J.; Hehre, W. J.; Binkley, J. S.; Gordon, M. S.; DeFrees, D. J.; Pople, J. A. *J. Chem. Phys.* **1982**, *77*, 3654−3665. (b) Rassolov, V. A.; Ratner, M. A.; Pople, J. A.; Redfern, P. C.; Curtiss, L. A. *J. Comput. Chem.* **2001**, *22*, 976−984.
(34) Barone, V.; Cossi, M. *J. Phys. Chem. A* **1998**, *102*, 1995−2001.
(35) (a) Abdur-Rashid, K.; Fong, T. P.; Greaves, B.; Gusev, D. G.; Hinman, J. G.; Landau, S. E.; Lough, A. J.; Morris, R. H. *J. Am. Chem. Soc.* **2000**, *122*, 9155−9171. (b) Rassolov, V. A.; Ratner, M. A.; Pople, J. A.; Redfern, P. C.; Curtiss, L. A. *J. Comput. Chem.* **2001**, *22*, 976−984.
(36) Bondi, A. *J. Phys. Chem.* **1964**, *68*, 441−451.

DOI: 10.1021/acs.inorgchem.5b00209
Inorg. Chem. XXXX, XXX, XXX−XXX